

1 ***MaUGT79* confers drought tolerance by regulating scopolin biosynthesis in plants**

2 Zhen Duan<sup>1</sup>, Fan Wu<sup>1</sup>, Qi Yan<sup>1</sup>, Shengsheng Wang<sup>1</sup>, Yimeng Wang<sup>1</sup>, Chris Stephen  
3 Jones<sup>2</sup>, Pei Zhou<sup>1</sup>, Caibin Zhang<sup>1</sup> and Jiyu Zhang<sup>1\*</sup>

4 <sup>1</sup>State Key Laboratory of Herbage Improvement and Grassland Agro-ecosystems, Key  
5 Laboratory of Grassland Livestock Industry Innovation, Ministry of Agriculture and  
6 Rural Affairs; College of Pastoral Agriculture Science and Technology, Lanzhou  
7 University, Lanzhou, 730020, China.

8 <sup>2</sup>Feed and Forage Development, International Livestock Research Institute, Nairobi  
9 00100, Kenya.

10 \* Corresponding author: zhangjy@lzu.edu.cn. Tel: +86 13893329958

11 **Abstract**

12 The coumarin scopoletin and its glycosylated form scopolin constitute a vast class of  
13 natural products that are considered to be high-value compounds, distributed widely in  
14 the plant kingdom, they help plants adapt to environmental stresses. However, the  
15 underlying molecular mechanism of how scopolin is involved in the regulation of plant  
16 drought tolerance remains largely unexplored. Here, UDP-glycosyltransferase 79  
17 (MaUGT79) was genetically mapped as the target gene by bulk segregant analysis  
18 sequencing (BSA-seq) from two *Melilotus albus* near-isogenic lines (NILs). MaUGT79  
19 exhibits glucosyltransferase activity toward scopoletin. The expression of *MaUGT79* is  
20 induced by drought stress and it was found to mediate scopolin accumulation and  
21 reactive oxygen species (ROS) scavenging under drought stress. Moreover, the  
22 transcription of *MaUGT79* was demonstrated to be directly and positively regulated by  
23 MaMYB4, which is a key integrator of both scopolin biosynthesis and drought  
24 tolerance. Collectively, this study reveals that MaMYB4 is a positive regulator in  
25 drought stress by targeting the *MaUGT79* promoter and activating its expression to  
26 coordinately mediate scopolin biosynthesis and drought tolerance, providing insights  
27 into the regulatory mechanism for plant growth adaption to environmental changes  
28 through accumulation of scopolin.

29 **Key words:** *MaUGT79*, *Melilotus albus*, scopolin biosynthesis, drought tolerance,  
30 MaMYB4, regulatory mechanism.

31 **Introduction**

32 In nature, plants are constantly exposed to various biotic threats and unfavorable  
33 growing conditions such as drought stress. To cope with drought stress, plants have  
34 evolved complex adaptive strategies. One such mechanism is the capacity to produce  
35 an impressive arsenal of stress-protective secondary metabolites (Sharma *et al.*, 2019;  
36 Stringlis *et al.*, 2019). Phenylpropanoids constitute a vast class of secondary  
37 metabolites that are considered to be high-value compounds due to their immense  
38 structural diversity and wide range of biological activities, and these compounds play  
39 important roles in the adaptation of plants to their environment (Doll *et al.*, 2018; Liu,  
40 Xinyu *et al.*, 2022). Coumarins, which are a rich source of medicines and therapeutic  
41 drugs, are important natural products of phenylpropane metabolism (Zhang *et al.*, 2005),  
42 and are thought to be beneficial to plants by conferring resistance to herbivorous insects  
43 (Alonso *et al.*, 2009) and pathogens (Perkowska *et al.*, 2021), facilitating nutrient  
44 uptake (Tsai & Schmidt, 2017; Robe *et al.*, 2021), shaping the composition of the root  
45 microbiome (Stringlis *et al.*, 2019; Voges *et al.*, 2019), and scavenging reactive oxygen  
46 species (ROS) (Doll *et al.*, 2018). Coumarin also has a beneficial health effect on the  
47 body in optimal consumption (Jakovljević Kovač *et al.*, 2021). However high  
48 concentrations of coumarin results in plants with poor palatability and dose-limiting  
49 toxicity (Liu *et al.*, 2010), which may be a major limiting factor for the use of forage  
50 legumes. Even so, coumarin metabolism is the focus of global attention due to a  
51 growing array of applications for its products, which have broad pharmacological  
52 prospectives and are commonly used in traditional spices and flavoring agents (Huang  
53 *et al.*, 2022). Consequently, there is a clear increasing trend in studies pertaining to the  
54 biosynthesis of coumarins (Tiwari *et al.*, 2016).

55 The biosynthetic pathway of the coumarin-glycoside scopolin branches off from the  
56 phenylpropanoid biosynthetic pathway at the level of the hydroxycinnamoyl-CoAs and  
57 cinnamoyl-CoAs. The coumarin scopoletin is produced from C2-hydroxylation of the  
58 hydroxycinnamoyl-CoA esters of the side-chain through 2-oxoglutarate- dependent  
59 dioxygenase feruloyl-CoA 6'-hydroxylase 1 (F6'H1) activity (Kai *et al.*, 2008) and then  
60 *trans-cis* isomerization and lactonization by the activity of COUMARIN SYNTHASE  
61 (COSY) (Vanholme *et al.*, 2019). Finally, scopoletin can be glycosylated by UDP-  
62 glycosyltransferases (UGT) to form scopolin in the cytoplasm (Le Roy *et al.*, 2016;  
63 Song *et al.*, 2018).

64 Glycosylation provides the plant with an easy way to modify molecules, the process  
65 plays an important role in regulating the solubility, stability and biological activity of  
66 various small molecules and it is closely related to drought stress responses of plants  
67 (Bowles *et al.*, 2005; Tognetti *et al.*, 2010). Glycosylation reactions are mediated by  
68 UDP-glycosyltransferases (UGTs) that catalyze the transfer of an activated nucleotide  
69 sugar to acceptor aglycones to form glycosides (Song *et al.*, 2018). Increasing evidence  
70 has indicated that *UGT* genes play pivotal roles in biosynthesis of phenolic compounds  
71 in many species (Dong *et al.*, 2020; Adiji *et al.*, 2021; Huang, X-X *et al.*, 2021)  
72 particularly in response to abiotic stresses (Rehman *et al.*, 2018). However, only a few  
73 coumarins and their corresponding UGTs have been functionally characterized due to  
74 the presence of hundreds of UGT-encoding genes in most plant species and the  
75 substrate promiscuity of UGT enzymes (Sun *et al.*, 2019; Krishnamurthy *et al.*, 2020).  
76 *Nicotiana tabacum* UGT73A1 and UGT73A2 have substrate specificity toward  
77 coumarins forming scopolin and esculin (Li *et al.*, 2001). *Tobacco-O-*  
78 *glucosyltransferase (TOGT)*-mediated glucosylation is required for scopoletin  
79 accumulation in cells surrounding tobacco mosaic virus (TMV) lesions, where this  
80 compound could both exert a direct antiviral effect and participate in reactive oxygen  
81 intermediate buffering (Chong *et al.*, 2002). The glycosylation activity of UGT73C7  
82 results in the redirection of phenylpropanoid metabolic flux to the biosynthesis of  
83 hydroxycinnamic acids and coumarins, promoting *SNC1*-dependent arabidopsis  
84 immunity (Huang, X-X *et al.*, 2021). Mounting evidence suggests that *UGT* is the key  
85 conduit for regulating coumarin biosynthesis in plants.

86 MYB transcription factors (TFs) belong to one of the largest and most important gene  
87 families, which regulate development under changing environmental conditions,  
88 primary and secondary metabolism, and plants response to stresses. Several members  
89 of the R2R3 MYB family have been reported to be involved in the biosynthesis of  
90 phenylalanine and phenylpropanoid-derived compounds (Chen *et al.*, 2019). MYB4 is  
91 reported to negatively regulate itself by binding to its own promoter (Zhao *et al.*, 2007).  
92 AtMYB7, a homolog of AtMYB4, repressed the expression of *UGT* genes that encode  
93 key enzymes in the flavonoid pathway (Fornale *et al.*, 2014). MYB72 regulates the  
94 biosynthesis of iron-mobilizing phenolic compounds, after which BGLU42 activity is  
95 required for their excretion into the rhizosphere (Stringlis *et al.*, 2018). One of the very  
96 few works dealing with the regulation of scopolin production by transcription factors

97 is about the antagonizing transcription factors MYB12, promoting flavonol synthesis,  
98 and MYB4, suppressing flavonol synthesis and thus promoting scopoletin production  
99 (Schenke *et al.*, 2011). However, the functions of MYB TFs in scopolin biosynthesis  
100 remains largely unknown, and the associated regulatory mechanisms is still a mystery.

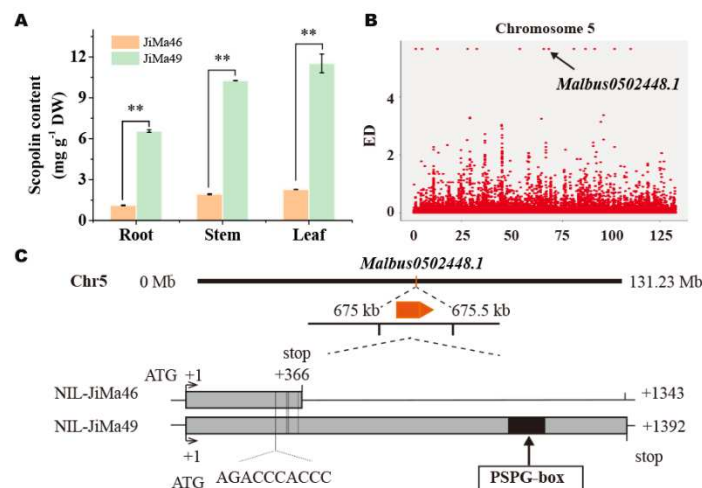
101 *Melilotus albus* is a diploid species with 8 chromosomes ( $2n=16$ ) and a sequenced  
102 genome of ~1.05 Gb (Wu *et al.*, 2022). It is an excellent rotation crop because it has  
103 been used for both forage production and soil improvement (Zabala *et al.*, 2018), and  
104 it is drought tolerant, winter hardy and grows in practically all soil types (Kulinich,  
105 2020). Coumarin content varies significantly among different *Melilotus* species (Nair  
106 *et al.*, 2010), and ranges from 0.2% to 1.3% of the dry matter within *M. albus* (Zhang  
107 *et al.*, 2018). Recent studies have suggested that coumarins play a crucial role in plant  
108 drought tolerance (Rangani *et al.*, 2020); however, the underlying molecular  
109 mechanisms are still largely unknown. For *M. albus*, most studies were about the  
110 conventional breeding of low coumarin content germplasm (Luo *et al.*, 2018; Zhang *et*  
111 *al.*, 2018) rather than deciphering the molecular mechanism. In our previous studies,  
112 differentially expressed unigenes and miRNAs involved in coumarin biosynthesis have  
113 been identified in *M. albus* (Luo *et al.*, 2017; Wu *et al.*, 2018). The *UGT* gene family  
114 of *M. albus* has been identified (Duan *et al.*, 2021). The key enzymes in the coumarin  
115 biosynthesis pathway have been identified in *M. albus* near-isogenic lines (NILs),  
116 JiMa46 and JiMa49 (Wu *et al.*, 2022). However, there has been little progress on  
117 functional analysis of coumarin biosynthesis genes. Therefore, filling the knowledge  
118 gap in molecular mechanisms of coumarin biosynthesis is particularly important.

119 In this study, we identified a UDP-glycosyltransferase encoding gene which was  
120 previously uncharacterised in *M. albus*, *MaUGT79*. We investigated the molecular  
121 functions of the *MaUGT79* gene in scopolin biosynthesis and drought tolerance through  
122 the generation and characterization of transgenic hairy roots over-expressing  
123 *MaUGT79*, as well as RNA interference (RNAi)-mediated knockdown of *MaUGT79*.  
124 We also found that MaMYB4 positively regulates the plants drought stress response  
125 through coordinately activating *MaUGT79*-involved scopolin biosynthesis. Our results  
126 unravel the mechanism of *MaUGT79*-mediated scopolin biosynthesis and drought  
127 tolerance, provide new genetic resources for enhancing drought tolerance in *M. albus*  
128 breeding and potentially contribute to sustainable agriculture in terms of weathering  
129 drought stresses.

130 **Results**

131 **An unknown UDP-glucosyltransferase, MaUGT, was genetically mapped based**  
132 **on the BSA-seq in *M. albus***

133 Scopolin contents in different tissues for two NILs (JiMa46 and JiMa49) of *M. albus*  
134 were analyzed by HPLC. Significantly higher levels of scopolin in leaf, stem and root  
135 were observed in JiMa49 than in JiMa46 (Figure 1A). To identify genes involved in the  
136 scopolin biosynthesis of *M. albus*, the BSA-seq was carried out. We found with high  
137 confidence that between JiMa46 and JiMa49, major polymorphic loci (SNPs and InDels)  
138 mapped at the 67,539,223 to 67,540,565 positions on chromosome 5, a region which  
139 was annotated as the UDP-glucosyltransferase (UGT) encoding gene *Malbus0502448.1*.  
140 This gene, with an unknown function, was assigned as the candidate gene underlying  
141 these loci (Figure 1B). We obtained the nomenclature-appropriate names of 189 full-  
142 length *UGT* genes based on chromosomal position from the *M. albus* genome (Duan et  
143 al., 2021), *Malbus0502448.1* is designated as *MaUGT79*. To further confirm the gene,  
144 the CDS of *MaUGT79* was amplified from JiMa46 and JiMa49 and the structures were  
145 analyzed. Sequence comparison among the UDP-glucosyltransferase encoding genes  
146 identified many nucleotide variations and InDels between the two NILs, which also  
147 exhibited frameshift mutations in the gene. *MaUGT79\_JiMa46* shows a ten-base  
148 deletion at the N-terminal region compared with *MaUGT79\_JiMa49*, which causes the  
149 early termination of *MaUGT79\_JiMa46* translation at the 121 amino acid position and  
150 the loss of the conserved Plant Secondary Product Glycosyltransferase (PSPG) box  
151 domain, while the full translation of *MaUGT79\_JiMa49* can proceed, generating a 463  
152 amino acid peptide (Figure 1C). Therefore, we assumed that the InDel which induced  
153 the premature termination of translation may affect protein function and thereby cause  
154 a loss of the *MaUGT79* gene function for glucosyltransferase in JiMa46. Hence, we  
155 considered that *MaUGT79* was the most likely candidate gene responsible for scopolin  
156 biosynthesis.



157

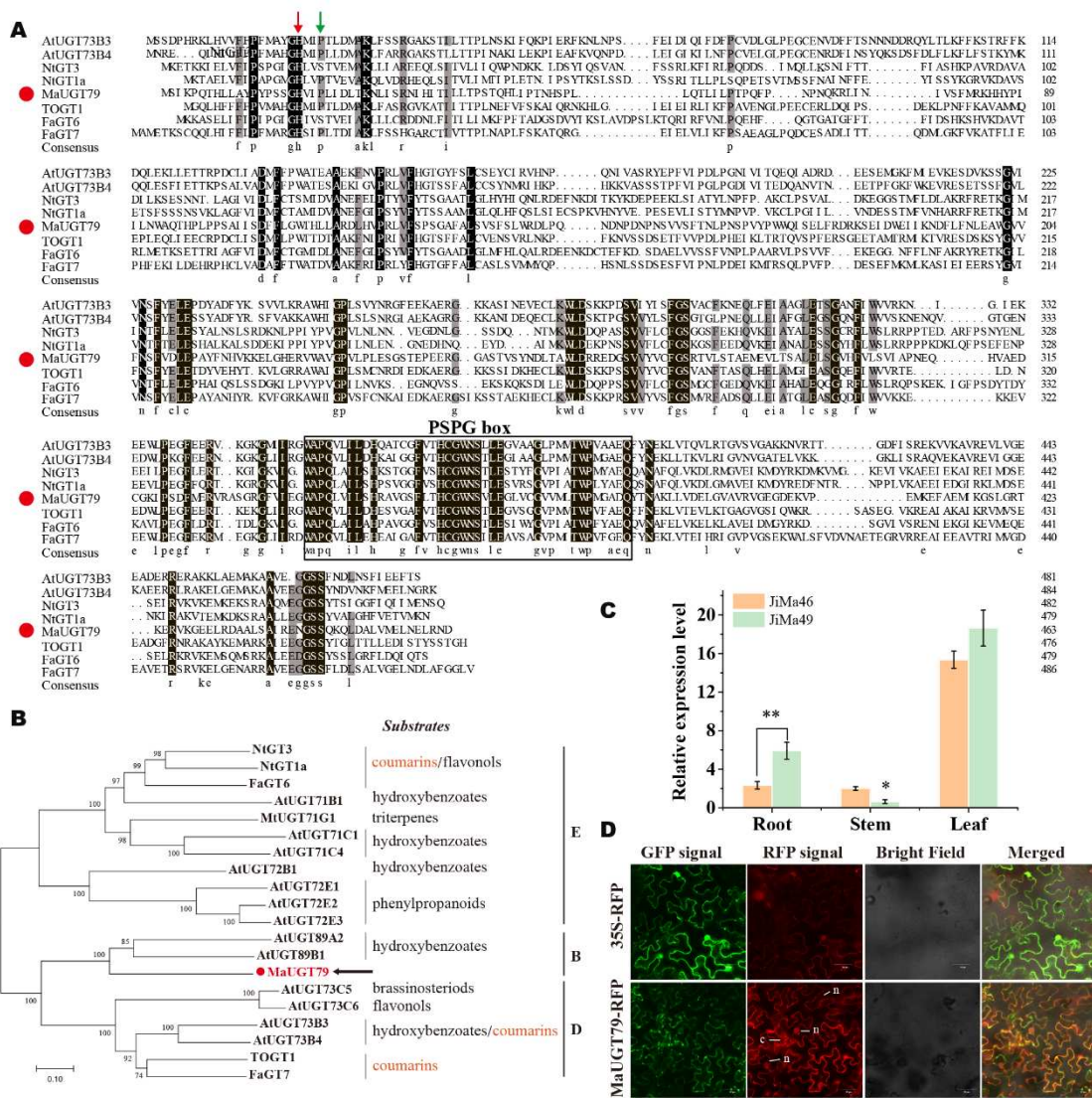
158 **Figure 1** Discovery of a specific scopolin UDP-glycosyltransferase in *M. albus*. A) Scopolin  
159 content in root, stem and leaf tissues of 2-month-old plants at the flowering stage of the two NILs,  
160 JiMa46 and JiMa49. The error bars indicate the SD values from at least three repetitions. Significant  
161 differences were detected by Student's t-test: \*\*,  $P < 0.01$ . B) Identification and localization of the  
162 scopolin biosynthesis locus between the two NILs based on BSA. The annotated gene was identified  
163 with SNPs and InDels between NILs JiMa46 and JiMa49. Each point represents an individual SNP  
164 locus. C) Physical position, gene structure, polymorphisms between JiMa46 and JiMa49 of  
165 *Malbus0502448.1*. Mutational changes in JiMa49 are indicated. Exon and the highly conserved  
166 plant secondary product glycosyltransferases (PSPG) box of plant glycosyltransferases are indicated  
167 in grey and black boxes, respectively. Nucleotide polymorphisms are indicated at their  
168 corresponding positions in the coding sequences.

169 *MaUGT79* contains a 1392 bp open reading frame (ORF) encoding a protein with a  
170 molecular mass of 51.86 kDa and a pI of 5.60. To further predict the function of  
171 *MaUGT79*, we aligned its protein sequence with similar previously characterized UGTs  
172 and carried out a phylogenetic analysis. Members of the UGT enzyme family consist  
173 of two similar (N- and C-terminal) domains, each possessing several alpha helices and  
174 beta strands (Adiji *et al.*, 2021). Multi-sequence alignment comparison analysis  
175 revealed that *MaUGT79* had high amino acid identity within the PSPG box 'WAPQ-  
176 2x-IL-x-H-5x-F-2x-HCGWNS-x-LE-4x-G-4x-TWP-4x-Q' near the C-terminal end  
177 (Figure 2A), which binds with the UDP portion of the sugar donor during catalysis. At  
178 the N-terminal region, *MaUGT79* possesses a critical catalytic His19 that is universally  
179 conserved across all plant UGTs. A neighboring residue, Pro22, was also identified that  
180 is either crucial for interacting with the acceptor substrate during catalysis or can partly  
181 define donor substrate acceptability (Shao *et al.*, 2005; Osman *et al.*, 2008) (Figure  
182 2A). In addition, we carried out phylogenetic analyses based on the amino acid  
183 sequences of *MaUGT79* and a set of UGTs that had been systematically screened for  
184 activity with a variety of hydroxylated benzoic acids, including coumarins (Song *et al.*,  
185 2016). Phylogenetic analysis indicated that *MaUGT79* clustered in the same branch as

186 AtUGT89B1 and AtUGT89A2, belonging to group B, which are closely related to  
187 group D that consists of known coumarin UGTs. UGT73B3 and UGT73B4 have been  
188 predicted as hydroxybenzoate glycosyltransferases, they readily glucosylate coumarins  
189 like their phylogenetic neighbors FaGT7 (Griesser *et al.*, 2008) and TOGT1 (Langlois-  
190 Meurinne *et al.*, 2005) (Figure 2B). Thus, the localization of MaUGT79 within this  
191 cluster would be consistent with a role in glycosylation of coumarin or other  
192 hydroxybenzoates.

193 **Cytoplasm and nuclei localized *MaUGT79* is highly expressed in *M. albus* leaf and  
194 root tissues**

195 The relative expression levels of *MaUGT79* in root, stem and leaf tissues between the  
196 genotypes JiMa46 and JiMa49 were analyzed (Figure 2C). The highest expression level  
197 was detected in leaf and root of JiMa49, where expression was significantly greater  
198 than in JiMa46, suggesting that *MaUGT79* may function in different tissues for the  
199 glycosylation process. We also examined the subcellular location of *MaUGT79* and  
200 found that the RFP signal was predominantly localized in the cytoplasm and nucleus  
201 (Figure 2D), suggesting a role for *MaUGT79* in scopolin metabolism in the cytoplasm.  
202 Certainly, the possibility of the partial diffusion of this protein back to the nuclei cannot  
203 be excluded.



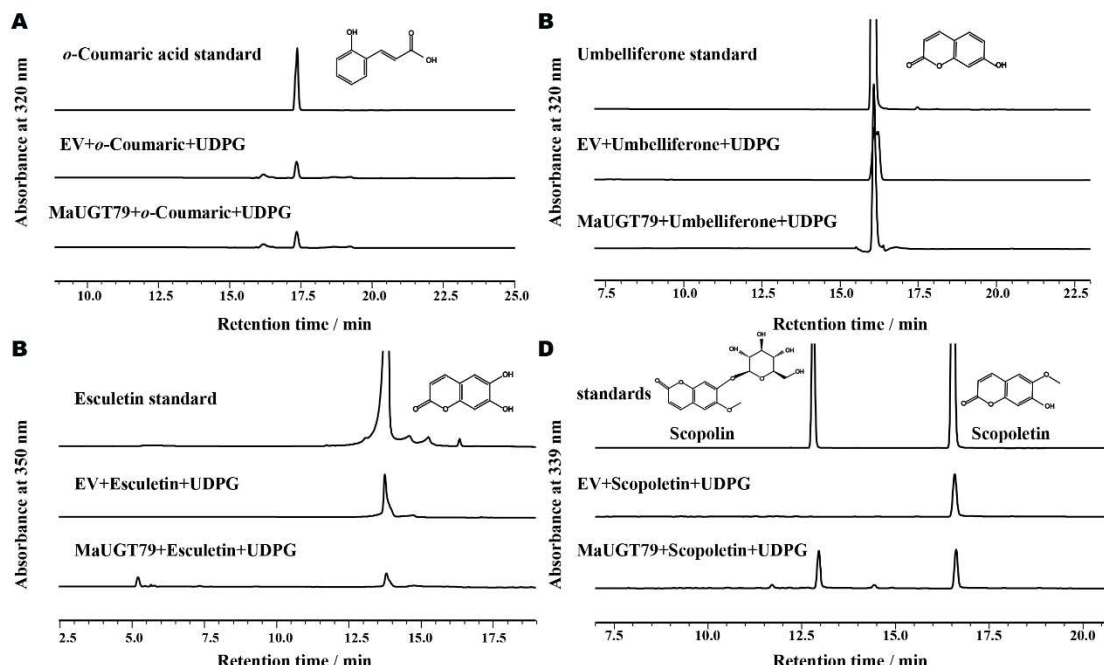
204

**Figure 2** Amino acid sequence alignment, phylogenetic analysis, subcellular localization of MaUGT79. A) Amino acid alignments of MaUGT79 with other identified UDP-glycosyltransferase (UGT) proteins involved in coumarin biosynthesis including AtUGT73B3, AtUGT73B4, NtGT3, NtGT1a, TOGT1, FaGT6 and FaGT7. The red arrow at the N-terminus indicates the presence of a critical catalytic His that is universally conserved across all plant UGTs. A neighboring residue, believed to be important in contributing to sugar donor recognition, is indicated by the green arrow. The black rectangle at the C-terminus indicates the domains of the PSPG box. Numbers indicate the last residue in each line. Identical residues are highlighted by a black background and similar residues are highlighted by a grey background. The red dots indicate MaUGT79. B) Phylogenetic tree of MaUGT79 together with other functionally characterized UGTs. The tree is constructed using the Neighbor-Joining method by the MEGA W software. Numbers indicate bootstrap values for 1000 replicates. The GenBank accession numbers of the UGT proteins are: AtUGT73B3 (AAL32831); AtUGT73B4 (BAE99671); NtGT3 (BAB88934); NtGT1a (BAB60720); TOGT1 (AAK28303); FaGT6 (ABB92748); FaGT7 (ABB92749); AtUGT71B1 (BAB02837); MtUGT71G1 (RHN56458); AtUGT71C1 (AAC35226); AtUGT71C4 (AAG18592); AtUGT72B1 (AAK25972); AtUGT72E1 (AAK83619); AtUGT72E2 (BAA97275); AtUGT72E3 (AAC26233);

221 AtUGT89A2 (CAB83309); AtUGT89B1 (AEE35520); AtUGT73C5 (AAD20156); AtUGT73C6  
222 (AAD20155). The red dot indicates MaUGT79. C) Relative expression levels of *MaUGT79* in root,  
223 stem and leaf tissues of 2-month-old plants at the flowering stage of the two NILs, JiMa46 and  
224 JiMa49. Data are normalized by  $\beta$ -tubulin. Data are shown as the mean (n = 3), and significant  
225 differences were detected by Student's t-test: \*, P<0.05 or \*\*, P<0.01. (d) The subcellular  
226 localization of MaUGT79 in *N. benthamiana* leaves. *MaUGT79* was fused to RFP. The fluorescence  
227 was observed under a confocal laser scanning microscope. Scale bars indicate 50  $\mu$ m.

228 **MaUGT79 exhibits scopoletin glucosyltransferase activity**

229 Previous studies have indicated that the amino acids in the N-terminal region of UGTs  
230 are crucial for interacting with the sugar acceptor substrate and that the PSPG box in  
231 the C-terminal region of UGTs plays a key role in sugar-donor binding (Osmani *et al.*,  
232 2009). MaUGT79 is a member of the UDP-dependent glycosyltransferase family,  
233 which mainly uses UDP-glucose as a sugar donor to catalyze the glucosylation of plant  
234 secondary metabolites (Gachon *et al.*, 2005; Bowles *et al.*, 2006). We thus  
235 heterologously expressed MaUGT79 in *E. coli* and purified the protein (Figure S1), and  
236 then conducted a substrate feeding assay using *o*-coumaric acid, esculetin,  
237 umbelliferone and scopoletin as the possible substrate, and UDP-glucose as a sugar  
238 donor to explore the ability of the recombinant protein to glucosylate coumarins. HPLC  
239 analysis of reaction products showed no new peaks were produced when using *o*-  
240 coumaric acid and umbelliferone as substrates, indicating that MaUGT79 could not  
241 catalyze the glucosylation of *o*-coumaric acid and umbelliferone. When using esculetin  
242 as a substrate, a small new peak was generated in the reaction products, suggesting that  
243 MaUGT79 had a weak catalytic capacity for esculetin. When scopoletin was used as a  
244 substrate, scopolin was produced with exactly the same retention time of 13 min as the  
245 scopolin authentic standard (Figure 3), indicating that MaUGT79 mainly had  
246 glucosylation activity against scopoletin and could catalyze the conversion of  
247 scopoletin to scopolin.



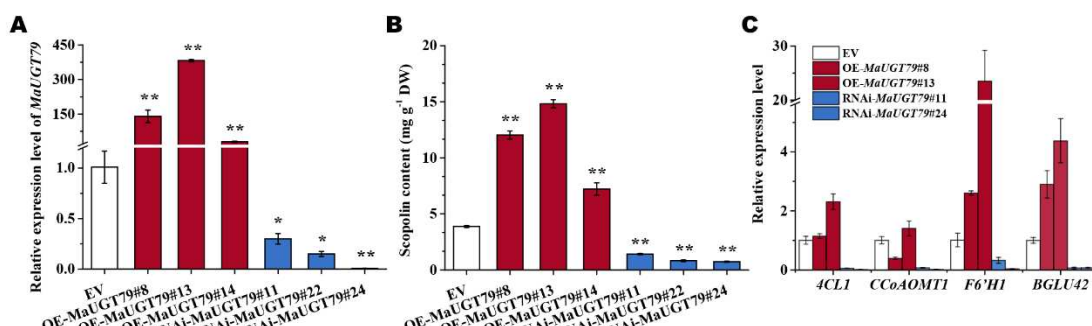
248

249 **Figure 3** The *in vitro* glucosylating activity of MaUGT79 toward different coumarins. HPLC  
250 analyses of the reaction products catalyzed by fusion protein MaUGT79 with *o*-coumaric acid A),  
251 umbelliferone B), esculetin C), scopoletin D) compared with authentic standards. UDP-glucose was  
252 used as the sugar donor. Empty vector was used as a negative control. The authentic *o*-coumaric  
253 acid, umbelliferone, esculetin, scopolin and scopoletin were used as the standards.

254 **MaUGT79 silencing decreased scopolin accumulation, while its overexpression  
255 enhanced scopolin biosynthesis**

256 Here, *A. rhizogenes*-mediated hairy root transformation was successfully developed in  
257 *M. albus* to further investigate whether *MaUGT79* contributes to scopoletin  
258 glucosylation *in vivo*. The transgenic hairy roots were identified by genomic PCR, RFP  
259 signal detection, and qRT-PCR (Figure S2, Figure 4A). Transgenic hairy root OE-  
260 *MaUGT79* lines with relatively high expression and RNAi lines with low expression  
261 were selected for functional characterization, while three independent *M. albus* hairy  
262 root lines that express the empty vector were used as a control (EV). The total  
263 endogenous scopolin from the OE-*MaUGT79* lines and RNAi lines was extracted and  
264 analyzed by HPLC. We found that the scopolin accumulation in OE-*MaUGT79* lines is  
265 much higher than that of EV lines. On the other hand, the scopolin level in RNAi lines  
266 was almost half that detected in EV lines (Figure 4B). These data indicate that  
267 *MaUGT79* catalyzes scopoletin glucosylation in *M. albus*. Then we assayed the  
268 expression levels of genes related to the phenylpropanoid pathway. As shown in Figure

269 4C, the expression levels of genes involved in the central phenylpropanoid pathway  
270 (*4CL1*, *CCoAOMT1*), and scopoletin biosynthesis (*F6'H1*, *BGLU42*) were obviously  
271 higher in OE-*MaUGT79* lines and reduced in RNAi lines compared with those in EV  
272 lines. We conclude that *MaUGT79* is indispensable for scopolin biosynthesis.

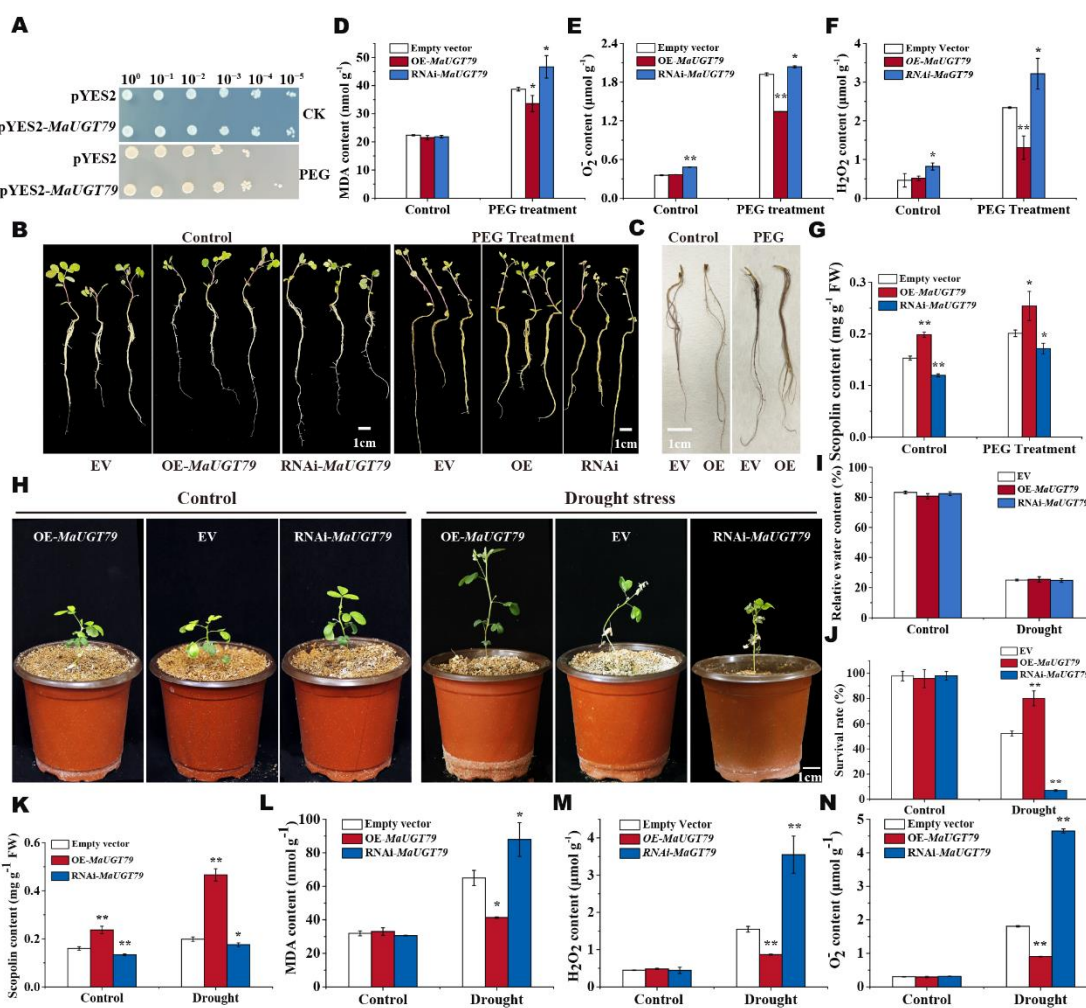


273 **Figure 4** Over- or knockdown expression of *MaUGT79* alters scopolin content in *M. albus* hairy roots. A) Analysis of *MaUGT79* expression levels and B) scopolin content in control (EV), overexpression (OE) and RNAi transgenic hairy roots. C) Gene expression levels of four scopolin biosynthesis genes (*4CL1*, *CCoAOMT1*, *F6'H1*, and *BGLU42*) in 21-d-old hairy roots. qRT-PCR was performed to detect gene expression levels. Data are normalized by  $\beta$ -tubulin. Data are shown as the mean (n=3). The error bars indicate the SD values from at least three repetitions. Significant differences were detected by Student's t-test: \*, P < 0.05 or \*\*, P < 0.01.

## 281 ***MaUGT79* contributes to drought stress tolerance through modulating scopolin 282 biosynthesis**

283 Coumarins are among the most bioactive plant secondary metabolites that serve as well-  
284 known antioxidants and show a response to drought stress by protecting plants against  
285 oxidative damage (Qin *et al.*, 2019; Rangani *et al.*, 2020; Patel *et al.*, 2021). Applied  
286 exogenous scopolin increased scopoletin and scopolin content (Figure S3A) and  
287 decreased the MDA and  $O_2^-$  content under 30% PEG6000 treatment and drought stress  
288 in EV and RNAi-*MaUGT79* hairy roots (Figure S3), indicating a positive role of  
289 scopolin reducing oxidative damage and promoting ROS scavenging under drought  
290 stress. Given that *MaUGT79* plays a significant role in modulating scopolin profiles,  
291 we asked whether *MaUGT79* is necessary for drought stress tolerance. First, an analysis  
292 of the expression of *MaUGT79* under drought stress was performed. We found that the  
293 expression of *MaUGT79* in *M. albus* was highly induced by 30% PEG treatment  
294 (Figure S4), and the conferring of drought tolerance by *MaUGT79* was confirmed in a  
295 yeast system (Figure 5A). To investigate how *MaUGT79* and its glycosylated scopolin

296 affect drought stress tolerance, transgenic hairy root OE-*MaUGT79* lines with  
297 relatively high expression and RNAi lines with low expression levels were selected for  
298 functional characterization, while transgenic hairy roots containing an empty vector  
299 were used as a control. No phenotypic differences were observed between the plants  
300 with OE-*MaUGT79* and RNAi-*MaUGT79* hairy roots and control plants under normal  
301 growth conditions (the relative water content was 82.13%). After 3 days of 30%  
302 PEG6000 treatment and 22 days for water-deficit treatment (the relative water content  
303 was 25.13%), the leaves of control plants displayed slight wilting and necrosis, the  
304 leaves of the plants with RNAi-*MaUGT79* transgenic hairy roots withered and were  
305 yellow, while no obvious damage was observed in the plants with *MaUGT79*-  
306 overexpressing transgenic hairy roots (Figure 5B, H). The survival rates of the plants  
307 with *MaUGT79*-overexpressing transgenic hairy roots were 75-86.67%, whereas only  
308 7.01% of RNAi-*MaUGT79* transgenic hairy roots plants survived. Control plants had a  
309 52.22% survival rate 22 days after drought stress induction (Figure 5J). Nitroblue  
310 tetrazolium (NBT) staining indicated that the control hairy roots displayed more severe  
311 damage in comparison with OE-*MaUGT79* hairy roots (Figure 5C), which was  
312 consistent with the result of O<sub>2</sub><sup>-</sup> content (Figure 5e, n). MDA and H<sub>2</sub>O<sub>2</sub> contents in OE-  
313 *MaUGT79* transgenic hairy roots decreased significantly relative to control hairy roots  
314 under 30% PEG6000 treatment and drought stress, while they increased in RNAi-  
315 *MaUGT79* transgenic hairy roots (Figure 5D, F, L, M). *MaUGT79*-overexpression lines  
316 treated with 30% PEG6000 and drought stress showed an increase in scopolin content  
317 and RNAi-*MaUGT79* lines showed a decreased scopolin content (Figure 5G, L).  
318 Therefore, we conclude that the reduced scopolin content in RNAi-*MaUGT79* hairy  
319 roots weakens the ROS scavenging activity and subsequently reduces drought tolerance.  
320 Consistently, drought marker genes, such as *MaCOR47*, *MaRD29A*, *MaLEA3*,  
321 *MaP5CS1*, *MaRD29B* and *MaDREB2B*, exhibited significantly elevated expression  
322 levels in two OE-*MaUGT79* lines upon exposure to 30% PEG6000 treatment (Figure  
323 S5).



324

**Figure 5** *MaUGT79* positively regulates drought tolerance in *M. albus* hairy roots. A) Drought stress tolerance analysis of *MaUGT79* in a yeast expression system compared with empty vector pYES2 (control) yeast. The two yeast cultures were independently grown in synthetic complete (SC)-Ura liquid medium containing 2% (m/v) galactose at 30 °C for 36 h up to  $A_{600}=0.4$ . Then, the yeast was collected and adjusted with SC-Ura including 2% galactose and cultivated up to  $A_{600}=1$  for stress analysis. The same number of cells was resuspended in 30% PEG6000. Then, serial dilutions ( $10^0$ ,  $10^{-1}$ ,  $10^{-2}$ ,  $10^{-3}$ ,  $10^{-4}$ ,  $10^{-5}$ ) were spotted onto SC-Ura agar plates and incubated at 30°C for 3 d. As a control, yeast with  $A_{600}=1$  without any stress was also spotted onto SC-Ura agar plates with the same dilutions as the treatments and grown at 30 °C for 3 d. B) Phenotypes of single seedling of overexpressing *MaUGT79* transgenic hairy roots (OE-*MaUGT79*), RNAi-*MaUGT79* transgenic hairy roots and transgenic hairy roots containing an empty vector (EV) grown under normal and 30% PEG6000 treatment for 3 days. C) Histochemical staining with NBT in hairy roots of EV and OE-*MaUGT79* under normal and 30% PEG6000 treatment for 3 days. (d-g) MDA content D),  $O_2^-$  content E),  $H_2O_2$  content F) and scopolin content G) in hairy roots of EV, OE-*MaUGT79* and RNAi-*MaUGT79* under normal and 30% PEG6000 treatment for 3 days. H) Phenotypes of single plant with OE-*MaUGT79*, RNAi-*MaUGT79* and EV transgenic hairy roots grown under normal and drought stress for 22 days. I) Relative water content of the plants with OE-*MaUGT79*, RNAi-*MaUGT79* and EV transgenic hairy roots under normal and drought stress at 22 days J),

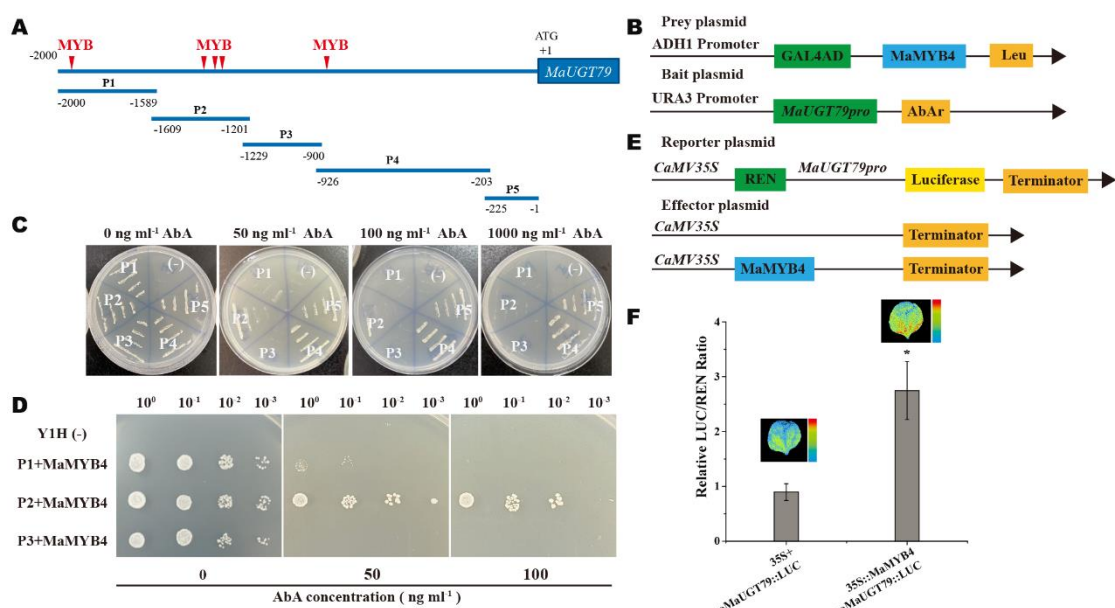
343 Survival rates of the plants with OE-*MaUGT79*, RNAi-*MaUGT79* and EV transgenic hairy roots  
344 grown under drought stress at 22 days, K-N) scopolin content K), MDA content L), O<sub>2</sub><sup>-</sup> content M),  
345 H<sub>2</sub>O<sub>2</sub> content N) in hairy roots of EV, OE-*MaUGT79* and RNAi-*MaUGT79* grown under normal  
346 and drought stress for 22 days. The error bars indicate the SD values from at least three repetitions  
347 of each treatment. Asterisks indicate significant differences between EV, OE-*MaUGT79* and RNAi-  
348 *MaUGT79* under the same growth conditions. Significant differences were detected by Student's t-  
349 test: \*, P<0.05 or \*\*, P<0.01.

350 **MaMYB4 activates *MaUGT79* expression through binding to its promoter**

351 To understand the transcriptional regulation of *MaUGT79*, the upstream promoter  
352 regions (2.0 kb in size) of *MaUGT79* genes were analyzed for the prediction of potential  
353 *cis*-elements. We found that the promoter region contained many MYB binding sites  
354 (Figure 6A). Numerous studies have clearly demonstrated that MYB transcription  
355 factors function as key regulators of plant secondary metabolism (Chen *et al.*, 2019).  
356 One of the very few works dealing with the regulation of scopolin production by  
357 transcription factors is about the AtMYB4 promotion of scopoletin production  
358 (Schenke *et al.*, 2011). So, a phylogenetic tree comprising the sequences of amino acids  
359 of AtMYB4 (At4g38620) and MYBs of *M. albus* identified previously (Chen *et al.*,  
360 2021) showed that *Malbus0702723.1* was most closely related to AtMYB4, as they  
361 shared 82.35% amino acid sequence identity (Figure S6A). We thus designated this  
362 protein as MaMYB4. qRT-PCR analysis also showed that the expression of MaMYB4  
363 was also induced by 30% PEG treatment (Figure S6B). The MaMYB4 transcript  
364 appeared mainly to be located in the nucleus (Figure S6D), which is consistent with its  
365 putative role as a transcription factor in the nucleus.

366 In order to confirm whether *MaUGT79* is regulated by MaMYB4, we first conducted a  
367 Y1H assay. A 2000-bp DNA sequence upstream of the *MaUGT79* start codon was  
368 separated into five parts, P1 (-2,000 to -1,589), P2 (-1,609 to -1,201), P3 (-1,229 to -  
369 900), P4 (-926 to -203), and P5 (-225 to -1, Figure 6A). We then integrated the P1, P2,  
370 P3, P4 and P5 sequences individually into the genomes of yeast cells. After introducing  
371 pGADT7-MaMYB4 into each of the respective yeast strains, we found that the P4 and  
372 P5 sequences of the *MaUGT79* promoter were not suitable for the Y1H system because  
373 1000 ng/mL AbA was still unable to suppress the basal expression in the Y1H Gold  
374 harbouring *P4MaUGT79*-AbAi and *P5MaUGT79*-AbAi (Figure 6C), and then only one  
375 strain, carrying the P2 promoter, was able to grow on selective media (Figure 6D). This  
376 indicated that MaMYB4 binds to the P2 fragments of the *MaUGT79* promoter.

377 Subsequently, a dual-luciferase reporter assay was performed to further verify whether  
 378 MaMYB4 activates the expression of *MaUGT79*. The *MaUGT79* promoter was used  
 379 to drive the luciferase (LUC) gene as fusion reporters, with MaMYB4 overexpressed  
 380 under the control of the CaMV 35S promoter as an effector (Figure 6E). As shown in  
 381 Figure 6f, the MaMYB4 and *MaUGT79* promoter co-transfected tobacco had a 2.7-fold  
 382 higher relative LUC/REN ratio than the control, supporting the concept of an interaction  
 383 between MaMYB4 and the *MaUGT79* promoter. Detection of LUC luminescence  
 384 indicated that co-expression with the MaMYB4 transcription factor increased the  
 385 expression of the *MaUGT79pro::LUC* reporters compared to the control lacking the  
 386 35S<sub>pro</sub>::MaMYB4 (Figure 6F). These results indicated that MaMYB4 can thus  
 387 transcriptionally up-regulate *MaUGT79*.



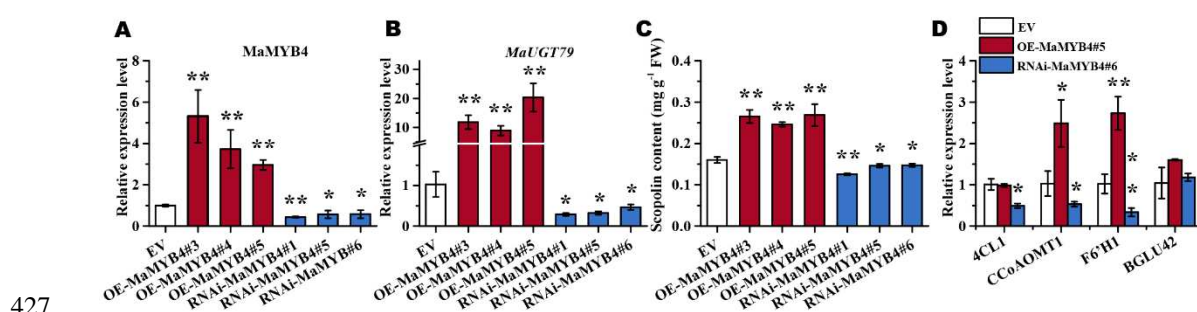
388

389 **Figure 6** The promoter of *MaUGT79* is the direct target of MaMYB4 (MYB, myeloblastosis). A) 390 Schematic diagram of the bait fragments (P1 to P5) used to construct the reporter vectors in the 391 yeast one-hybrid assay. The red triangles indicate MYB binding sites. B) Schematic diagram of the 392 prey plasmid and bait plasmid in yeast one-hybrid (Y1H) assay. The promoter fragment of 393 *MaUGT79* was cloned into the pAbAi vector to generate the bait plasmid and the prey plasmid was 394 generated by recombining the MaMYB4 gene into the pGADT7 vector. C) Transcriptional 395 activation analysis of Y1H Gold [*Pro1/2/3/4/5/MaUGT79-pAbAi*]. D) Yeast one-hybrid assay. A 396 pair of plasmids, pAbAi containing different fragments of the *MaUGT79* promoter and pGADT7 397 containing MaMYB4 were introduced into yeast strain Y1H gold and cultured on SD medium 398 without Leu containing different concentrations of AbA at 30°C for 3 days. E) Schematic diagram 399 of the reporter plasmid and effector plasmid. The promoter fragment of *MaUGT79* was cloned into 400 the pGreenII 0800-LUC vector to generate the reporter plasmid. The effector plasmid was generated 401 by recombining the MaMYB4 gene into an overexpression vector (pBI 121). F) Dual-luciferase

402 (LUC) assay in *N. benthamiana* leaves showing that MaMYB4 activates transcription of *MaUGT79*  
403 promoters. The leaves infiltrated with the empty vector and *MaUGT79pro::LUC* as a control.  
404 Representative photographs were taken (above), and LUC/Renilla Luciferase (REN) activity  
405 detection to verify that MaMYB4 activates the transcription of *MaUGT79* (below). The error bars  
406 indicate the SD values from the mean of at least five repetitions. Significant differences were  
407 detected by Student's t-test: \*,  $P < 0.05$ .

408 **MaMYB4 positively regulates *MaUGT79*-mediated scopolin accumulation and**  
409 **drought tolerance**

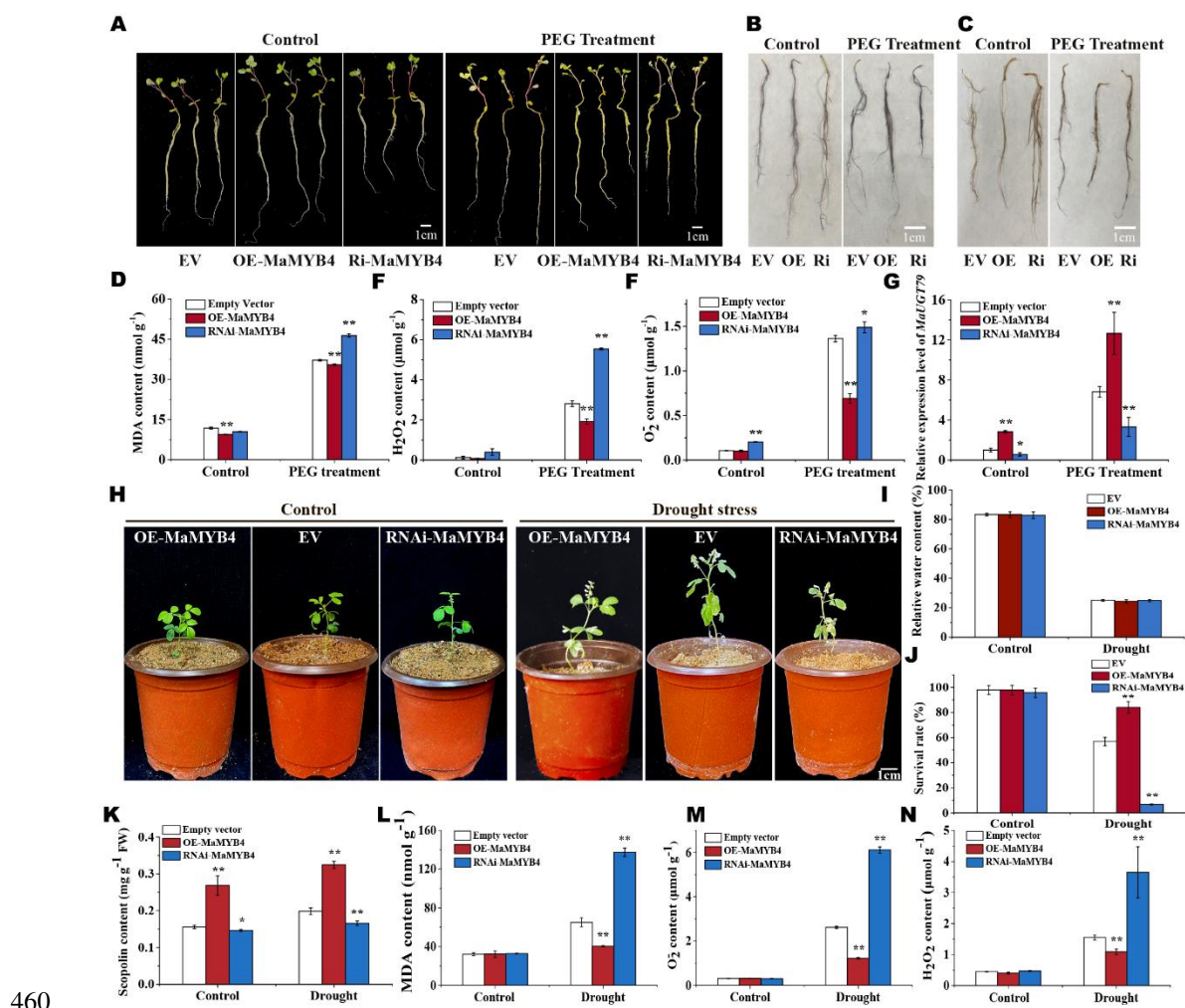
410 In order to explore the MaMYB4 expression profiles of *M. albus*, qRT-PCR was  
411 performed to assess transcript accumulation in different tissues. MaMYB4 was highly  
412 expressed in the leaves, which was positively correlated with the expression of  
413 *MaUGT79* (Figure S6B) and was induced by drought stress (Figure S6C). In order to  
414 gain further understanding of the regulatory roles of MaMYB4, overexpression and  
415 RNAi transgenic hairy roots were generated (Figure 7). qRT-PCR confirmed that the  
416 transgenic hairy roots accumulated high levels of MaMYB4 transcripts (2.9- to 5.3-fold;  
417 Figure 7A), which in turn increased the expression levels of *MaUGT79* by 8.9- to 20.4-  
418 fold (Figure 7B). Scopolin content increased by 1.66-, 1.54-, and 1.68-fold in  
419 comparison to the controls, respectively (Figure 7C). RNAi transgenic hairy roots  
420 exhibited low expression levels of MaMYB4 (0.43- to 0.58- fold), which in turn  
421 decreased the expression levels of *MaUGT79* by 0.29- to 0.47- fold. Scopolin content  
422 decreased by 0.91-, 0.78- and 0.92- fold compared with the controls, respectively.  
423 Interestingly, the transcription of *CCoAOMT1* and *F6'H1* genes involved in scopolin  
424 biosynthesis were obviously enhanced in OE-MaMYB4 lines and declined in RNAi  
425 lines (Figure 7D). Taken together, these findings support the assumption that MaMYB4  
426 is a positive factor that modulates scopolin biosynthesis.



428 **Figure 7** MaMYB4 positively regulates scopolin content in *M. albus* hairy roots. (MYB,  
429 myeloblastosis). A-B) Quantitative reverse-transcription (qRT)-PCR analysis of MaMYB4 A) and

430 *MaUGT79* B) in control (EV), OE-MaMYB4 and RNAi-MaMYB4 transgenic hairy roots. C)  
431 Scopolin content in control (EV), OE-MaMYB4 and RNAi-MaMYB4 transgenic hairy roots. D)  
432 Gene expression levels of four scopolin biosynthesis genes (*4CL1*, *CCoAOMT1*, *F6'H1*, and  
433 *BGLU42*) in 21-d-old hairy roots. qRT-PCR was performed to detect gene expression levels. Data  
434 are normalized by  $\beta$ -tubulin. The error bars indicate the SD values from the mean of at least three  
435 repetitions. Significant differences were detected by Student's t-test: \*,  $P<0.05$  or \*\*,  $P<0.01$ .

436 Further, OE-MaMYB4 and RNAi-MaMYB4 transgenic hairy roots were selected to  
437 investigate whether MaMYB4 plays a role in drought tolerance, where transgenic hairy  
438 roots containing an empty vector were used as the control (EV). The EV, OE and RNAi  
439 transgenic hairy roots were subjected to 30% PEG6000 treatments for 3 days and water-  
440 deficit treatment for 22 days (the relative water content was 24.72%). Expectedly, the  
441 plants with OE-MaMYB4 transgenic hairy roots had significantly improved drought  
442 tolerance, while more severe wilting and necrosis of the leaves were observed in the  
443 plants with RNAi transgenic hairy roots compared with the EV (Figure 8A, H). The  
444 survival rates of the plants with MaMYB4-overexpressing transgenic hairy roots were  
445 78.57-86.67%, whereas only 6.69% of RNAi-MaMYB4 transgenic hairy roots plants  
446 survived. Control plants had a 56.83% survival rate 22 days after drought stress was  
447 applied (Figure 5J), which was evidenced by the results of NBT and DAB staining  
448 (Figure 8B, C), and MDA,  $H_2O_2$  and  $O_2^-$  contents (Figure 8D-F, L-N). In addition, after  
449 30% PEG6000 treatment, the expression level of *MaUGT79* in OE-MaMYB4  
450 transgenic hairy roots was significantly up-regulated, while it was significantly  
451 inhibited in RNAi-MYB4 transgenic hairy roots (Figure 8G), indicating that MaMYB4  
452 expression was up-regulated under drought stress and MaMYB4 activates *MaUGT79*  
453 expression. Accordingly, the content of scopolin increased significantly under drought  
454 stress in OE-MaMYB4 transgenic hairy roots (Figure 8K). Consistently, drought  
455 marker genes, such as *MaCOR47*, *MaRD29A*, *MaLEA3*, *MaP5CSI*, *MaRD29B* and  
456 *MaDREB2B*, exhibited significantly higher expression levels in OE-MaMYB4 hairy  
457 roots and lower expression levels in RNAi-MaMYB4 hairy roots upon exposure to 30%  
458 PEG6000 treatment (Figure S7). Taken together, these results indicated that MaMYB4  
459 also plays a positive role in drought tolerance.



461 **Figure 8** MaMYB4 positively regulates drought tolerance in *M. albus* hairy roots. A) Phenotypes  
462 of single seedling of overexpressing MaMYB4 transgenic hairy roots (OE-MaMYB4), RNAi-  
463 MaMYB4 transgenic hairy roots and transgenic hairy roots transferring an empty vector (EV) under  
464 normal and 30% PEG6000 treatment for 3 days. B-C) Histochemical staining with NBT B) and  
465 DAB C) in hairy roots of EV, OE- MaMYB4 and RNAi- MaMYB4 under normal and 30% PEG6000  
466 treatment for 3 days. D-G) MDA content D),  $\text{H}_2\text{O}_2$  content E),  $\text{O}_2^-$  content F) and *MaUGT79*  
467 expression level G) in hairy roots of EV, OE-MaMYB4 and RNAi- MaMYB4 under normal and  
468 30% PEG6000 treatment for 3 days. H) Phenotypes of single plants with OE-MaMYB4, RNAi-  
469 MaMYB4 and EV transgenic hairy roots under normal and drought stress for 22 days. I) Relative  
470 water content of plants with OE- MaMYB4, RNAi- MaMYB4 and EV transgenic hairy roots under  
471 normal and drought stress at 22 days J), Survival rates of plants with OE-MaMYB4, RNAi-  
472 MaMYB4 and EV transgenic hairy roots grown under drought stress at 22 days, K-N) scopolin  
473 content K), MDA content L),  $\text{O}_2^-$  content M),  $\text{H}_2\text{O}_2$  content N) in hairy roots of EV, OE-MaMYB4  
474 and RNAi-MaMYB4 grown under normal and drought stress for 22 days. The error bars indicate  
475 the SD values from at least three repetitions of each treatment. Asterisks indicate significant  
476 differences between EV, OE-MaMYB4 and RNAi-MaMYB4 under the same growth conditions.  
477 Significant differences were detected by Student's t-test: \*,  $P<0.05$  or \*\*,  $P<0.01$ .

478 **Discussion**

479 Using BSA based on 122,318 SNPs obtained from two NILs, JiMa46 and JiMa49 (Wu  
480 *et al.*, 2022), we successfully identified a single polymorphic locus in a gene associated  
481 with scopolin biosynthesis that is located on chromosome 5, which we name as  
482 *MaUGT79*. To provide further insight into the genetic function and regulation  
483 mechanism of *MaUGT79*, we performed transgenic assays, substrate feeding assays  
484 and molecular biology experiments to demonstrate that *MaUGT79* functions as a  
485 positive regulator in scopolin biosynthesis of *M. albus* and enhances tolerance to  
486 drought stress. Our findings also highlight the regulatory function of a MYB  
487 transcription factor, MaMYB4, in scopolin biosynthesis and drought tolerance, and  
488 provide important insights into the regulatory mechanism underlying scopolin  
489 accumulation and drought tolerance in *M. albus*.

490 **The contribution of *MaUGT79* to drought stress tolerance is closely associated  
491 with scopolin accumulation**

492 Previous studies have localized the global fluorescence of scopolin in leaf, stem, and  
493 root and found that coumarins move throughout the plant body via the xylem sap and  
494 it is a highly complex and dynamic process (Robe *et al.*, 2021). Our result showed  
495 higher levels of scopolin in leaf, stem and root of *M. albus*. In Arabidopsis, BGLU42  
496 was shown to be responsible for the deglycosylation of scopolin (Stringlis *et al.*, 2018),  
497 but which is responsible for the glycosylation of scopolin is unknown (Robe *et al.*, 2021).

500 In our study, *MaUGT79* encodes a UDP-glycosyltransferase that grouped in the same  
501 phylogenetic clade as AtUGT89B1 and AtUGT89A2, which belong to group B in our  
502 analysis (Figure 2B). AtUGT89A2 is a key factor that affects the differential  
503 accumulation of dihydroxybenzoic acid glycosides in arabidopsis (Chen & Li, 2017).  
504 A previous study showed that known coumarin UGTs, belonging to groups D  
505 (Langlois-Meurinne *et al.*, 2005) and E (Huang, X-X *et al.*, 2021), are more likely to  
506 be responsible for coumarin glycosylation modification. The group B protein, which is  
507 closely related to group D and E, in *M. albus* led us to propose *MaUGT79* as a major  
508 candidate gene for coumarin biosynthesis. Transgenic OE-*MaUGT79* in *M. albus* hairy  
509 roots indeed showed significantly increased scopolin accumulation (Figure 4). In  
Arabidopsis, scopolin accumulation in leaves was also reported in response to biotic  
and abiotic stresses (Doll *et al.*, 2018). So we then closely examined the effects of

510 overexpression of *MaUGT79* in response to drought stress. We first confirmed the  
511 positive role of scopolin in drought stress by reducing oxidative damage and promoting  
512 ROS scavenging (Figure S3). Then we found that the OE-*MaUGT79* lines displayed no  
513 obvious damage compared with the EV control under 30% PEG treatment and water-  
514 deficit treatment for 22 days (Figure 5B, H). In addition, OE-*MaUGT79* had  
515 significantly decreased MDA (Figure 5D, L), O<sub>2</sub><sup>·</sup> (Figure 5E, N), and H<sub>2</sub>O<sub>2</sub> (Figure 5F,  
516 M) contents, and increased scopolin content (Figure 5G, K) compared with the EV  
517 under 30% PEG6000 treatment and drought stress treatment. Further to this, the RNAi-  
518 *MaUGT79* transgenic lines showed an opposite trend (Figure 5D-F, L-N). We speculate  
519 that increased drought tolerance may be conferred by the correlated *MaUGT79*-  
520 mediated scopolin accumulation. Similar effects of coumarin-accumulation on  
521 increased abiotic stress have been reported in *Salvadora persica*, rice (*Oryza sativa*)  
522 and peanut (*Arachis hypogaea*) (Qin *et al.*, 2019; Rangani *et al.*, 2020; Patel *et al.*,  
523 2021). We conclude that the increased scopolin content in OE-*MaUGT79* hairy roots  
524 strengthens the ROS scavenging activity of the *M. albus* hairy roots and subsequently  
525 increases drought tolerance.

526 **Glycosylation of scopoletin promotes scopoletin biosynthesis via feedback  
527 activation of scopoletin biosynthesis genes**

528 In our study, we observed that *MaUGT79* overexpression lines had greatly upregulated  
529 expression of critical genes encoding enzymes involved in scopoletin biosynthesis,  
530 including *4CL1*, *CCoAOMT1*, *F6'H1* and *BGLU42*, whereas the knock-down lines of  
531 *MaUGT79* had decreased transcription of these genes. These findings demonstrate that  
532 glycosylation of scopoletin accelerated the biosynthesis of the scopoletin, and that this  
533 is closely correlated with the upregulation of the biosynthesis genes. A previous study  
534 showed that overexpression of *TOGT*, a scopoletin glucosyltransferase, in tobacco  
535 results in both scopoletin and scopolin over-accumulation as compared to wild-type  
536 (Gachon *et al.*, 2004), suggesting that up-regulation of glycosylating activity toward a  
537 specific substrate does not necessarily result in lower accumulation of the  
538 corresponding aglycone form. So, we believe that as the plant cells continuously  
539 consume aglycones upon constitutive expression of *MaUGT79*, they require more  
540 substrate, which in turn stimulates the expression of the upstream enzyme encoding  
541 genes and accelerated biosynthesis of scopoletin.

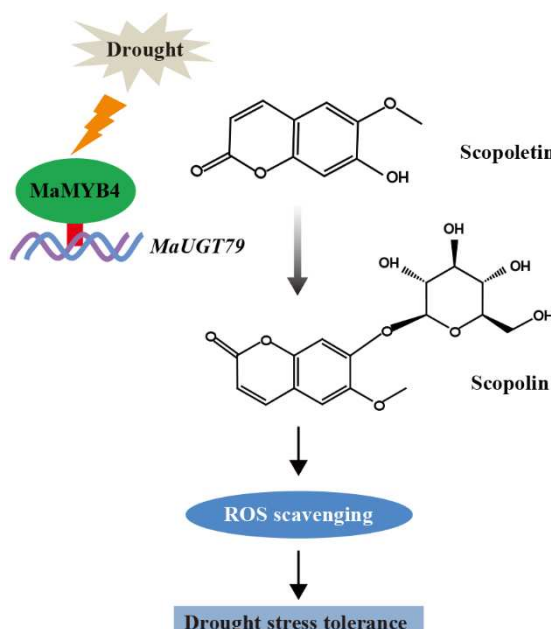
542 **MaMYB4 is linked to scopolin metabolism via *MaUGT79* in regulating drought**  
543 **stress adaption**

544 Transcription factors (TFs) are a group of regulators that play crucial roles in many  
545 plant biological and developmental processes by regulating gene expression at the  
546 transcriptional level through recognition of specific DNA sequences in promoters  
547 (Mitsuda & Ohme-Takagi, 2009). Although the biosynthesis of scopolin is most  
548 responsive to MaUGT79 activity in *M. albus*, knowledge of the mechanisms involved  
549 in the regulation of *MaUGT79* transcription is fairly limited. The TF MYB15 is  
550 proposed to regulate the basal synthesis of scopoletin (Chezem *et al.*, 2017). MYB72,  
551 which tightly regulates *F6'H1* expression, is also involved in scopolin accumulation  
552 (Stringlis *et al.*, 2018). In this study we identified a MYB TF, MaMYB4, whose  
553 expression closely correlates with *MaUGT79* gene expression (Figure S6), with  
554 overexpression leading to an increase in scopolin (Figure 7C). In grapes (*Vitis vinifera*),  
555 VvMYB4b, VvMYB4a, and VvMYB4-like were associated with reduced  
556 proanthocyanidin and anthocyanin accumulation and, down-regulation of structural and  
557 regulatory genes of the flavonoid biosynthesis pathway (Cavallini *et al.*, 2015; Ricardo  
558 Perez-Diaz *et al.*, 2016). In *A. thaliana*, AtMYB4 and AtMYB7 are two members in  
559 subgroup 4 of the R2R3-MYB transcription factors, overexpression of AtMYB4  
560 reduces the expression of AtMYB7, and the lack of AtMYB7 results in an increase in  
561 the expression of the early phenylpropanoid genes *C4H*, *4CL*, and *UGT* (Fornale *et al.*,  
562 2014). These findings suggest that a variety of MYB4 sequences in different plant  
563 species are involved in various metabolic mechanisms, and thus a new function in  
564 regulating scopolin biosynthesis is presented in this study. We identified that MaMYB4  
565 could directly control the expression of *MaUGT79*, a glycosyltransferase involved in  
566 modulating scopolin biosynthesis. Over-expression of MaMYB4 significantly  
567 enhanced the expression of *MaUGT79*, the content of scopolin and drought tolerance,  
568 and these levels were reduced when MaMYB4 was down-regulated via RNA-  
569 interference (Figure 8). Yeast one-hybrid (Y1H) and Dual-luciferase (LUC) assays  
570 showed that MaMYB4 acts by binding to the promoter of *MaUGT79* and activates  
571 *MaUGT79* transcription (Figure 6). These results link MaMYB4 to the scopolin  
572 biosynthetic pathway in improving drought stress tolerance through activating the  
573 expression of *MaUGT79*. Here, we add new knowledge about upstream regulatory  
574 factors of *MaUGT79*, which show developmental-based expression to stimulate

575 scopolin accumulation and drought tolerance in *M. albus*.

576 In summary, we show that *MaUGT79* over-expression in *M. albus* hairy roots resulted  
577 in increased scopolin accumulation, leading to enhanced drought tolerance. Furthermore,  
578 we show that *MaMYB4* over-expression promotes the deposition of scopolin by  
579 directly regulating the expression of *MaUGT79*. Under drought conditions, *MaMYB4*  
580 expression is higher and *MaMYB4* directly activates the expression of *MaUGT79*.  
581 *MaUGT79* catalyses the conversion of scopoletin to scopolin, leading to an increase in  
582 scopolin content. The resulting accumulation of scopolin contributes to drought  
583 tolerance by increasing ROS scavenging capacity (Figure 9).

584



585

586 **Figure 9** A proposed mechanistic model for the drought-dependent regulation of scopolin  
587 biosynthetic *MaUGT79* gene expression, regulated by *MaMYB4* in *M. albus*. Under drought  
588 conditions, *MaMYB4* is up-regulated and activates the expression of *MaUGT79*. *MaUGT79*  
589 catalyses the conversion of scopoletin to scopolin, which results in an increase in scopolin content.  
590 The accumulation of scopolin leads to drought tolerance by increasing ROS scavenging.

## 591 Materials and methods

### 592 Plant materials and growth conditions

593 *M. albus* plants were grown in an illuminated incubator under controlled conditions (16  
594 h/8 h day/night cycle at 25°C, with a relative humidity of 40%). Roots, stems, leaves,

595 and flowers at the flowering stage were collected, frozen in liquid nitrogen and then  
596 stored at -80°C until use. *Nicotiana benthamiana* plants used in this study were grown  
597 in pots in a growth chamber under a 16 h photoperiod with a 20°C: 25°C, night: day  
598 temperature.

599 **Bulked-segregant analysis sequencing (BSA-seq)**

600 BSA-seq analysis was performed on the NILs to identify the target gene in this study.  
601 The two bulks consisted of the JiMa46 pool with an extremely low scopolin content  
602 phenotype and the JiMa49 pool with an extremely high scopolin content phenotype,  
603 and they were constructed by mixing an equal amount of DNA extracted from 30  
604 individuals of JiMa46 and JiMa49 plants, respectively. SNP discovery was performed  
605 as described in a previous study (Wu *et al.*, 2022).

606 **Gene cloning and sequence analysis**

607 A 1343 bp and 1392 bp CDS of *MaUGT79* from JiMa46 and JiMa49, respectively, was  
608 amplified based on the genome data using Phanta Max Super-Fidelity DNA Polymerase  
609 (Vazyme Biotech Co.,Ltd, Nanjing). Gene specific primers (Table S1) were designed  
610 using DNAMAN software (Wang, 2015). The CDS was confirmed by sequencing. For  
611 phylogenetic analysis, the deduced amino acid sequences of MaUGT79 were aligned  
612 with previously characterized UGTs using multiple sequence comparison by ClustalX  
613 (Larkin *et al.*, 2007) . The phylogenetic tree was constructed based on the alignments  
614 using MEGA 7.0 (Kumar *et al.*, 2016) with the neighbour-joining (NJ) method, and  
615 bootstrap tests were performed using 1,000 replicates to support statistical reliability.  
616 A 2.0 kb sequence of the promoters of *MaUGT79* was cloned and used to identify the  
617 *cis*-acting elements in the promoter regions through the PlantCARE website  
618 (<http://bioinformatics.psb.ugent.be/webtools/plantcare/html/>) (Lescot *et al.*, 2002).

619 **Subcellular localization assay**

620 To investigate the subcellular localization of MaUGT79, we constructed a recombinant  
621 MaUGT79 tagged at the N-terminus with red fluorescent protein (RFP), and the CDS  
622 of *MaUGT79* was inserted between the *Xba*I and *Bam*HI sites of the binary vector  
623 pBI121 DsRed2 (Wu *et al.*, 2022) with expression driven by the CaMV 35S promoter.  
624 The specific primers are listed in Table S1. The leaves of 6-week-old *N. benthamiana*  
625 seedlings were selected for a transient overexpression experiment, *Agrobacterium*

626 *tumefaciens* strain GV3101 carrying 35S:*MaUGT79*-RFP and the control vector with  
627 RFP alone were transformed into the leaves according to a previous report (Liu,  
628 Xiaoying *et al.*, 2022). The cytoplasm marker pBI-NLS-CFP was co-transformed into  
629 the *N. benthamiana* leaves to exhibit the location of the cytoplasm. The system was  
630 subsequently cultured in the dark for one day and then in daylight for another two days.  
631 A laser scanning confocal microscope (Olympus FV3000, Japan) was used to observe  
632 the image of transformed leaves.

633 **Heterologous protein expression and substrate feeding**

634 The *MaUGT79* coding sequence was inserted between the *Bam*HI and *Sac*I sites of the  
635 pET32a vector (Duan *et al.*, 2021) using the ClonExpress® MultiS One Step Cloning  
636 Kit (Vazyme Biotech Co.,Ltd, Nanjing) following the protocol provided. Primers are  
637 shown in Table S1. The construct was then transformed into *Escherichia coli* strain  
638 BL21 (DE3) (TransGen Biotech, Beijing). After incubation at 37°C in Luria– Bertani  
639 (LB) liquid medium containing ampicillin (100 µg ml<sup>-1</sup>) for 24 h, the culture was diluted  
640 and grown until the optical density at 600nm (OD600) of the cultured cells reached 0.6-  
641 0.8. After adding 0.1 mM isopropyl-β-D-thiogalactopyranoside (IPTG) the culture was  
642 incubated at 16°C and 180 rpm for 20 h to induce expression of the recombinant protein  
643 (Sun *et al.*, 2017). The protein was then purified using *Proteinlso*® Ni-NTA Resin  
644 (TransGen Biotech, Beijing) and analyzed on a 12% SDS-PAGE gel.

645 The BL21 (DE3) cells harboring the pET32a-*MaUGT79* vector and empty vector were  
646 cultured in the same conditions for *E. coli* expression. Afterwards, IPTG (final  
647 concentration of 0.1 mM) was added and incubated for 20 h, then the substrate *o*-  
648 coumaric acid, esculetin, umbelliferone, scopoletin (final concentration of 0.1 mM) and  
649 500 mM UDP-Glucose (98%, Innochem Co., Ltd) were added, and the culture was  
650 incubated for 24 h. After that, the reaction system was extracted with an equal amount  
651 of ethyl acetate. The recovered ethyl acetate extract was decompressed and dried, then  
652 dissolved in MeOH for high-performance liquid chromatography (HPLC) analysis  
653 (Yang *et al.*, 2016). The detection wavelength of *o*-coumaric acid and umbelliferone  
654 was 320 nm, the detection wavelength of esculetin was 350 nm, and the detection  
655 wavelength of scopoletin and scopolin was 346 nm.

656 **Validation of Heterologous Expression in Yeast**

657 To produce the pYES2-*MaUGT79* construct, the full-length coding sequence of

658 *MaUGT79* was amplified from JiMa49 and inserted between the *Bam*HI and *Xba*I sites  
659 of the pYES2 (Duan *et al.*, 2021) expression vector using a ClonExpress® MultiS One  
660 Step Cloning Kit following the manufacturer's protocol with the specific primers listed  
661 in Supplementary Table S1. Following confirmation of the cloned sequence, the  
662 recombinant pYES2-*MaUGT79* plasmid and empty pYES2 plasmid were transformed  
663 into *Saccharomyces cerevisiae* strain INVSc1 (Duan *et al.*, 2021). The two yeast  
664 cultures were independently grown in synthetic complete (SC)-Ura liquid medium  
665 containing 2% (*m/v*) galactose at 30°C for 36 h up to an OD600 of 0.4. Then, the yeasts  
666 were harvested and adjusted with SC-Ura including 2% galactose and cultivated up to  
667 an OD600 of 1.0 for stress analysis. The same amount of cells were resuspended in 30%  
668 PEG 6000 (Zhang *et al.*, 2021). The treated yeast liquid was diluted 1:10 and cultured  
669 on SC-U/2% (*w/v*) glucose agar plates for 2–3 days to observe colony growth, and  
670 photos were taken to record the expression of the binding protein.

671 **Yeast one-hybrid assay**

672 For Matchmaker Gold yeast one-hybrid system (Clontech, Mountain View, CA, USA),  
673 the MaMYB4 CDS was fused to the GAL4 transcription factor activation domain  
674 (GAL4AD) in the pGADT7 vector (Zheng *et al.*, 2021) to generate the prey vector  
675 (pGADT7-MaMYB4). While the various promoter fragments of *MaUGT79* (2.0-kb)  
676 were inserted into the pAbAi vector (Zheng *et al.*, 2021) to construct the baits  
677 (*pro1/2/3/4/5MaUGT79-AbAi*). These *Bst*BI-cut bait constructs were integrated  
678 separately into the genome of Y1HGold (Zheng *et al.*, 2021) to generate five bait  
679 reporter strains. The minimal inhibitory concentrations of abscisic acid (AbA) were  
680 determined for the baits using SD/-Ura agar plates containing 0–1000 ng ml<sup>-1</sup> AbA.  
681 After selecting the transformants on SD/-Ura plates, the pGADT7-MaMYB4 construct  
682 was introduced into the bait reporter strains, with a blank pGADT7 plasmid serving as  
683 a negative control. Positive transformants were selected on SD/-Leu medium  
684 supplemented with an appropriate concentration of AbA and cultured at 30°C for 3 d  
685 (Zheng *et al.*, 2021).

686 **Dual-luciferase assay**

687 For the dual-luciferase (Dual-LUC) assay, the *MaUGT79* promoter (-1609~-1 bp) was  
688 ligated into pGreenII-0080-LUC (Zheng *et al.*, 2021) to generate the reporter construct  
689 *proMaUGT79:LUC*. The MaMYB4 CDS was ligated into the binary vector pBI121 to

690 generate the effector construct *35S:MaMYB4*. The effector and reporter constructs were  
691 transformed into *A. tumefaciens* strain GV3101 harbouring the pSoup helper vector  
692 (Nguyen *et al.*, 2021), respectively, which were further co-infected into 6-week-old *N.*  
693 *benthamiana* leaves. The leaves were infiltrated with the pBI121 effector construct and  
694 the *proMaUGT79:LUC* as a control (Zheng *et al.*, 2021). The injected tobacco plants  
695 were kept in the dark for 12 hours and then 2 days in normal light conditions. A  
696 Fluorescence Chemiluminescence Imaging System (FX6.EDGE Spectra; VILBER,  
697 France) was used to capture the LUC image. The promoter activities were determined  
698 by measuring Firefly Luciferase to Renilla Luciferase (LUC/REN) ratios using the Dual  
699 Luciferase Reporter Gene Assay Kit (RG027, Beyotime, Shanghai, China) with a  
700 Multimode Reader (Varioskan LUX, Thermo Fisher, Finland). Five biological  
701 replications were measured for each sample.

702 **Vector construction and *Agrobacterium rhizogenes*-mediated transformation  
703 system of *M. albus***

704 To produce the *MaUGT79* and *MaMYB4* overexpression and RNAi expression  
705 constructs, the full-length cDNAs of *MaUGT79* and *MaMYB4* were cloned into the  
706 binary vectors pBI121 and pK7GWIWG2 (II) RR, using the ClonExpress<sup>®</sup> MultiS One  
707 Step Cloning Kit and Gateway LR Clonase Enzyme Mix (Invitrogen), respectively. The  
708 constructs were introduced into *A. rhizogenes* strain K599 by the electroporation  
709 method (Wang *et al.*, 2021). Transgenic hairy roots were obtained according to a  
710 previous report (Wang *et al.*, 2021). The transgenic hairy root lines containing the  
711 overexpression empty vector (EV) were used as a control. All transgenic lines were  
712 tested by PCR and RFP visualization to identify positive lines. The transgenic hairy  
713 roots were then transferred to Murashige & Skoog medium (with 100 mg ml<sup>-1</sup>  
714 cefotaxime) and maintained in the dark, at 22°C, for two months. Hairy roots were then  
715 harvested for determination of scopolin content (Figure S2a).

716 **Drought stress and exogenous scopolin treatments and tolerance evaluation**

717 In order to investigate the changes in *MaUGT79* expression under drought stress, six-  
718 week-old plants were treated with 30% PEG6000. The leaf samples for qRT-PCR  
719 analysis were harvested at 0, 3, and 24 h after treatment. All samples were immediately  
720 frozen in liquid nitrogen and stored at -80°C. Three replicates were performed for each  
721 sample. For *M. albus* hairy root drought experiments, the 2-month-old EV, OE-

722 *MaUGT79/MaMYB4* and *RNAi-MaUGT79/MaMYB4* transgenic hairy roots lines  
723 were treated with 30% PEG6000 for three days. And the EV and *RNAi-MaUGT79* lines  
724 were also treated with 30% PEG6000+100  $\mu$ M scopolin for three days. Moreover, after  
725 18 days growth of the plants with transgenic hairy roots, the seedlings from each line  
726 were carefully transferred to flowerpots containing vermiculite and sand ( $v/v = 1:1$ ) for  
727 30 days of growth and then the seedlings were used in the phenotyping experiment. The  
728 plants grown under water-replete conditions were watered twice per week with 1/2  
729 Hoagland nutrient solution. For drought tolerance comparisons, water was withheld  
730 from *MaUGT79/MaMYB4*-overexpressing, *MaUGT79/MaMYB4*-silencing and  
731 control lines as in Zhang *et al.* (2012) for 22 days until there were distinguishable  
732 differences between control lines and *MaUGT79/MaMYB4*-overexpressing or  
733 *MaUGT79/MaMYB4*-silencing lines. At least 30 plants per independent line were  
734 evaluated in each treatment, and all treatments were repeated three times.

### 735 **RNA extraction and gene expression analysis**

736 Total RNA was extracted from leaves, stems and roots at the flowering stage and from  
737 hairy roots of *M. albus* using the TransZol reagent (TransGen Biotech, Beijing). First  
738 strand cDNA was obtained using the Hifair® III 1st Strand cDNA Synthesis SuperMix  
739 for qPCR (gDNA digester plus) by oligo(dT) primer (Yeasen biotech Co., Ltd.,  
740 Shanghai). Quantitative RT-PCR was performed using Hieff® qPCR SYBR® Green  
741 Master Mix (No Rox) (Yeasen biotech Co., Ltd., Shanghai) on a CFX96 Real-Time  
742 PCR Detection System (Bio-Rad, Los Angeles, CA, USA).  $\beta$ -tubulin was used as a  
743 housekeeping reference gene. The expression levels were calculated relative to the  
744 reference and determined using the  $2^{-\Delta\Delta CT}$  method (Zong *et al.*, 2021). There were three  
745 biological replicates for all analyses. Primers used for qRT-PCR are listed in Table S1.

### 746 **Scopolin extraction and quantification**

747 For scopolin extraction, ambient temperature-dried samples derived from fresh samples  
748 were ground and passed through a sieve with an aperture size of 0.45 mm and extracted  
749 with an ethanol/water mixture (80: 20,  $v/v$ ). For tissue extraction, 50 ml of solvent  $g^{-1}$   
750 of dry weight was used. For hairy roots extraction, 5 ml of 80% ethanol per 100 mg  
751 was added to the frozen material (Doll *et al.*, 2018). After shaking for 10 min, ultrasonic  
752 extraction was performed at room temperature for 60 min. The ratio between the weight  
753 of the fresh samples and the volume of the extraction solution was the same for all

754 samples in a given experiment. The extracts were filtered through 0.45  $\mu\text{m}$  filters for  
755 high performance liquid chromatography (HPLC) analysis.

756 HPLC separation was performed on an Agilent 1100 HPLC system using a 5  $\mu\text{m}$  C18  
757 column (4.6 mm  $\times$  150 mm, Agilent-XDB), maintained at 30°C, with water (containing  
758 0.1% phosphorous acid) and acetonitrile as the mobile phase. The flow rate of the  
759 mobile phase was set at 1 ml  $\text{min}^{-1}$  over 20 min. For the quantification of scopolin, the  
760 calibration was performed with an eight-point calibration curve made using commercial  
761 sources of scopolin and scopoletin (Chengdu PureChem-Standard Co., Ltd) (Figure S7).  
762 Chemicals used in this study were of analytical or HPLC grade.

### 763 **Measurement of physiological and histochemical staining**

764 For physiological analyses, *M. albus* plants were treated with 30% PEG6000 for 3 days.  
765 Histochemical staining of  $\text{O}_2^-$  was conducted by the BCIP/NBT Chromogen Kit  
766 (Solarbio, Beijing, China). The MDA,  $\text{O}_2^-$  and  $\text{H}_2\text{O}_2$  content were measured using the  
767 detection kit (Solarbio, Beijing, China) according to the manufacturer's instructions,  
768 respectively (Huang, X *et al.*, 2021). Histochemical staining of  $\text{H}_2\text{O}_2$  was conducted  
769 using the DAB Chromogen Kit (Solarbio, Beijing, China).

### 770 **Data Availability statement**

771 The genomic data of *M. albus* are openly available in NCBI (NCBI BioProject ID  
772 PRJNA674670).

### 773 **Acknowledgments**

774 This work was financially supported by the National Natural Science Foundation of  
775 China (32061143035, 32271752), Inner Mongolia Seed Industry Science and  
776 Technology Innovation Major Demonstration Project (2022JBGS0040), the  
777 Fundamental Research Funds for the Central Universities (lzujbky-2022-ey17).

778 *Conflict of interest statement.* The authors declare that they have no competing interests.

### 779 **Author contributions**

780 JZ, ZD, FW and QY designed the experiment and conception; ZD, YW, SW, PZ and  
781 CZ performed experiments; ZD, FW, QY, SW, YW, CZ and JZ analyzed data. ZD, QY  
782 and SW wrote the manuscript. JZ and CSJ revised the manuscript. All authors read and  
783 approved the manuscript.

### 784 **Supplemental data**

785 **Supplemental Table S1** List of primers used in the present study.

786 **Supplemental Figure S1** SDS-PAGE analysis of MaUGT79 heterologously expressed  
787 in *E. coli*. Expression of the protein in *E. coli* BL21(DE3) was induced by IPTG for 20  
788 h at 16°C. M, protein molecular size markers; Lane 1, empty vector; Lane 2, induction  
789 of MaUGT79; Lane 3, purified MaUGT79 protein.

790 **Supplemental Figure S2** Phenotype and identification of transgenic hairy roots. A)  
791 Phenotype of transgenic hairy roots. B) Genomic DNA (gDNA) PCR identification of  
792 35S:*MaUGT79* in transgenic *M. albus* hairy roots using 35S-F/RED-R primers shown  
793 in supplementary table. C) RFP signals in *MaUGT79*-overexpressing hairy roots of *M.*  
794 *albus*.

795 **Supplemental Figure S3** A) HPLC profiling of scopolin and scopoletin in control (EV),  
796 overexpression lines (OE-1 and OE-5), and RNAi lines (RNAi-1 and RNAi-6) under  
797 30% PEG6000 treatment and applied with exogenous scopolin after 30% PEG6000  
798 treatment. Authentic scopolin and scopoletin were used as standards. B-C) MDA  
799 content B) and O<sub>2</sub><sup>-</sup> content C) in hairy roots of EV and RNAi-*MaUGT79* under control  
800 (CK), 30% PEG6000 treatment and 30% PEG6000+scopolin treatment for 3 days. The  
801 error bars indicate the SD values from the mean of at least three repetitions of each  
802 treatment (\*, *P* < 0.05 or \*\*, *P* < 0.01).

803 **Supplemental Figure S4** Expression pattern of *MaUGT79* under 30% PEG6000  
804 treatment using qRT-PCR. The values shown are the means ± standard deviation of  
805 three replicates.  $\beta$ -tubulin was used as a normalization control for qRT-PCR. Red lines  
806 indicate the expression values (FPKM) from RNA-seq data. CK represents the control.

807 **Supplemental Figure S5** Expression levels of drought marker genes including  
808 *MaCOR47* A), *MaRD29A1* B), *MaLEA3* C), *MaP5CS1* D), *MaRD29B* E) and  
809 *MaDREB2B* F) in hairy roots of EV and two OE-*MaUGT79* lines (OE-*MaUGT79*#1  
810 and OE-*MaUGT79*#5) under control and 30% PEG6000 treatment for 3 days.  $\beta$ -tubulin  
811 was used as a control for qRT-PCR. The error bars indicate the SD values from the  
812 mean of at least three repeats of each treatment. Asterisks indicate significant

813 differences (\*,  $P < 0.05$  or \*\*,  $P < 0.01$ ) between EV and OE-MaUGT79 under the same  
814 growth conditions based on Student's *t*-test.

815 **Supplemental Figure S6** Correlation and phylogenetic analysis of MaMYB4. A)  
816 Phylogenetic analysis of the amino acid sequences of AtMYB4 (At4g38620) and  
817 MYBs of *M. albus*. Gene ID for labels can be found in supplementary table. B) The  
818 correlation between the expression of MaMYB4 and *MaUGT79* in different tissues of  
819 *M. albus* at the flowering stage. Error bars represent  $\pm$  SD (n=3). C) Expression pattern  
820 of MaMYB4 under 30% PEG6000 treatment using qRT-PCR. The values shown are  
821 the means  $\pm$  standard deviation of three replicates.  $\beta$ -tubulin was used as the reference  
822 gene. D) The subcellular localization of MaMYB4. MaMYB4 was fused to RFP into  
823 *N. benthamiana* leaves. The fluorescence was observed under a confocal laser scanning  
824 microscope. The cyan signal of NLS (nuclear localization signal)-CFP shows the  
825 location of the nuclear marker. Scale bars indicate 50  $\mu$ m.

826 **Supplemental Figure S7** Expression levels of drought marker genes including  
827 *MaCOR47* A), *MaRD29A1* B), *MaLEA3* C), *MaP5CS1* D), *MaRD29B* E) and  
828 *MaDREB2B* F) in hairy roots of EV, OE-MaMYB4 and RNAi-MaMYB4 under control  
829 and 30% PEG6000 treatment when grown for 3 days.  $\beta$ -tubulin was used as  
830 normalization controls for qRT-PCR. The error bars indicate the SD values from at least  
831 three repeats of each treatment. Asterisks indicate significant differences (\*,  $P < 0.05$  or  
832 \*\*,  $P < 0.01$ ) between EV, OE-MaMYB4 and RNAi-MaMYB4 under the same growth  
833 conditions based on Student's *t*-test.

834 **Supplemental Figure S8** The calibration curve of scopolin.

835 **References**

836  
837 **Adiji OA, Docampo-Palacios ML, Alvarez-Hernandez A, Pasinetti GM, Wang X, Dixon RA.**  
838 UGT84F9 is the major flavonoid UDP-glucuronosyltransferase in *Medicago truncatula*. Plant  
839 Physiol. 2021; **185**(4): 1617-1637. 10.1093/plphys/kiab016  
840 **Alonso C, Garcia IM, Zapata N, Perez R.** Variability in the behavioural responses of three generalist  
841 herbivores to the most abundant coumarin in *Daphne laureola* leaves. Entomol. Exp. Appl. 2009:

842 **132**(1): 76-83. <http://doi.10.1111/j.1570-7458.2009.00869.x>

843 **Bowles D, Isayenkova J, Lim EK,Poppenberger B** Glycosyltransferases: managers of small molecules.

844 Curr. Opin. Plant Biol. 2005: **8**(3): 254-263. <http://doi.10.1016/j.pbi.2005.03.007>

845 **Bowles D, Lim E-K, Poppenberger B, Vaistij FE.** Glycosyltransferases of lipophilic small molecules.

846 Annu. Rev. Plant Biol. 2006: **57**567-597. <http://doi.10.1146/annurev.arplant.57.032905.105429>

847 **Cavallini E, Tomas Matus J, Finezzo L, Zenoni S, Loyola R, Guzzo F, Schlechter R, Ageorges A, Arce-Johnson P, Tornielli GB.** The phenylpropanoid pathway is controlled at different branches by a set of R2R3-MYB C2 repressors in Grapevine. Plant Physiol. 2015: **167**(4): 1448-U1552. <http://doi.10.1104/pp.114.256172>

851 **Chen C, Zhang K, Khurshid M, Li J, He M, Georgiev MI, Zhang X, Zhou M.** MYB transcription

852 repressors regulate plant secondary metabolism. Crit. Rev. Plant Sci. 2019: **38**(3): 159-170.

853 <http://doi.10.1080/07352689.2019.1632542>

854 **Chen H-Y, Li X.** Identification of a residue responsible for UDP-sugar donor selectivity of a

855 dihydroxybenzoic acid glycosyltransferase from *Arabidopsis* natural accessions. Plant J. 2017:

856 **89**(2): 195-203. <http://doi.10.1111/tpj.13271>

857 **Chen L, Wu F, Zhang J.** NAC and MYB families and lignin biosynthesis-related members identification

858 and expression analysis in *Melilotus albus*. Plants. 2021: **10**(2): 303. <http://doi.10.3390/plants10020303>

860 **Chezem WR, Memon A, Li F-S, Weng J-K, Clay NK.** SG2-Type R2R3-MYB transcription factor

861 MYB15 controls defense-induced lignification and basal immunity in *Arabidopsis*. Plant Cell.

862 2017: **29**(8): 1907-1926. <http://doi.10.1105/tpc.16.00954>

863 **Chong J, Baltz R, Schmitt C, Beffa R, Fritig B, Saindrenan P.** Downregulation of a pathogen-

864 responsive tobacco UDP-Glc: phenylpropanoid glucosyltransferase reduces scopoletin

865 glucoside accumulation, enhances oxidative stress, and weakens virus resistance. Plant Cell.

866 2002: **14**(5): 1093-1107. <http://doi.10.1021/cen-v077n039.p064>

867 **Doll S, Kuhlmann M, Rutten T, Mette MF, Scharfenberg S, Petridis A, Berreth D-C, Mock H-P.**

868 Accumulation of the coumarin scopolin under abiotic stress conditions is mediated by the

869 *Arabidopsis thaliana* THO/TREX complex. Plant J. 2018: **93**431-444. <http://doi.10.1111/tpj.13797>

871 **Dong N-Q, Sun Y, Guo T, Shi C-L, Zhang Y-M, Kan Y, Xiang Y-H, Zhang H, Yang Y-B, Li Y-C.**

872 UDP-glucosyltransferase regulates grain size and abiotic stress tolerance associated with

873 metabolic flux redirection in rice. Nat. Commun. 2020: **11**(1): 1-16. <http://doi.10.1038/s41467-020-16403-5>

875 **Duan Z, Yan Q, Wu F, Wang Y, Wang S, Zong X, Zhou P, Zhang J.** Genome-Wide analysis of the

876 UDP-Glycosyltransferase family reveals its roles in coumarin biosynthesis and abiotic stress in

877 *Melilotus albus*. Int. J. Mol. Sci. 2021: **22**(19): 10826. <http://doi.10.3390/ijms221910826>

878 **Fornale S, Lopez E, Salazar-Henao JE, Fernandez-Nohales P, Rigau J, Caparros-Ruiz D.** AtMYB7,

879 a new player in the regulation of UV-sunscreens in *Arabidopsis thaliana*. Plant Cell Physiol.

880 2014: **55**(3): 507-516. <http://doi.10.1093/pcp/pct187>

881 **Gachon C, Baltz R, Saindrenan P.** Over-expression of a scopoletin glucosyltransferase in *Nicotiana*

882 *tabacum* leads to precocious lesion formation during the hypersensitive response to tobacco

883 mosaic virus but does not affect virus resistance. Plant Mol. Biol. 2004: **54**(1): 137-146.

884 <http://doi.10.1023/B:PLAN.0000028775.58537.fe>

885 **Gachon CMM, Langlois-Meurinne M, Saindrenan P.** Plant secondary metabolism

886 glycosyltransferases: the emerging functional analysis. Trends Plant Sci. 2005: **10**(11): 542-549.  
887 http://doi. 10.1016/j.tplants.2005.09.007

888 **Griesser M, Vitzthum F, Fink B, Bellido ML, Raasch C, Munoz-Blanco J, Schwab W.** Multi-  
889 substrate flavonol O-glucosyltransferases from strawberry (*Fragaria x ananassa*) achene and  
890 receptacle. J. Exp. Bot. 2008: **59**(10): 2611-2625. http://doi. 10.1093/jxb/ern117

891 **Huang S, Wang M, Mao D, Rasool A, Jia C, Yang P, Han L, Yan M.** Isolation, identification and  
892 characterization of growth parameters of *Pseudomonas putida* HSM-C2 with coumarin-  
893 degrading bacteria. 2022: **27**(18): 6007.

894 **Huang X-X, Wang Y, Lin J-S, Chen L, Li Y-J, Liu Q, Wang G-F, Xu F, Liu L, Hou B-K** The novel  
895 pathogen-responsive glycosyltransferase UGT73C7 mediates the redirection of  
896 phenylpropanoid metabolism and promotes *SNC1*-dependent *Arabidopsis* immunity. *The Plant*  
897 *journal*, 2021a: 10.1111/tpj.15280

898 **Huang X-X, Zhu G-Q, Liu Q, Chen L, Li Y-J, Hou B-K.** Modulation of plant salicylic acid-associated  
899 immune responses via glycosylation of dihydroxybenzoic acids. *Plant Physiol.* 2018: **176**(4):  
900 3103-3119. http://doi. 10.1104/pp.17.01530

901 **Huang X, Cao L, Fan J, Ma G, Chen L.** CdWRKY2-mediated sucrose biosynthesis and CBF-signalling  
902 pathways coordinately contribute to cold tolerance in bermudagrass. *Plant Biotechnol. J.* 2021b:  
903 1-16. http://doi. 10.1111/pbi.13745

904 **Jakovljević Kovač M, Mihajlović L, Molnar MJCJOFS, Technology.** Coumarin in grounded  
905 cinnamon and teas containing cinnamon-extraction and determination by HPLC method. *Sci.*  
906 *Technol. Food Ind.* 2021: **13**(2): 246-252.

907 **Kai K, Mizutani M, Kawamura N, Yamamoto R, Tamai M, Yamaguchi H, Sakata K, Shimizu BI.**  
908 Scopoletin is biosynthesized via ortho-hydroxylation of feruloyl CoA by a 2-oxoglutarate-  
909 dependent dioxygenase in *Arabidopsis thaliana*. *Plant J.* 2008: **55**(6): 989-999. http://doi.  
910 10.1111/j.1365-313X.2008.03568.x

911 **Krishnamurthy P, Tsukamoto C, Ishimoto M.** Reconstruction of the evolutionary histories of *UGT*  
912 gene superfamily in Legumes clarifies the functional divergence of duplicates in specialized  
913 metabolism. *Int. J. Mol. Sci.* 2020: **21**(5): 10.3390/ijms21051855

914 **Kulinich RA.** Seed productivity of yellow clover depending on planting dates and method of sowing in  
915 the central steppe of the Crimea. *Taurida Herald of the Agrarian Sciences.* 2020: (2): 73-80.  
916 http://doi. 10.33952/2542-0720-2020-2-22-73-80

917 **Kumar S, Stecher G, Tamura K.** MEGA7: molecular evolutionary genetics analysis version 7.0 for  
918 bigger datasets. *Molecular biology evolution.* 2016: **33**(7): 1870-1874. http://doi.  
919 10.1093/molbev/msw054

920 **Langlois-Meurinne M, Gachon CMM, Saindrenan P.** Pathogen-responsive expression of  
921 glycosyltransferase genes *UGT73B3* and *UGT73B5* is necessary for resistance to *Pseudomonas*  
922 *syringae* pv tomato in *Arabidopsis*. *Plant Physiol.* 2005: **139**(4): 1890-1901. http://doi.  
923 10.1104/pp.105.067223

924 **Larkin MA, Blackshields G, Brown NP, Chenna R, Mcgettigan PA, Mcwilliam H, Valentin F,**  
925 **Wallace IM, Wilm A, Lopez R.** Clustal W and Clustal X version 2.0. *Bioinformatics*, 2007:  
926 **23**(21): 2947-2948. http://doi. 10.1093/bioinformatics/btm404

927 **Le Roy J, Huss B, Creach A, Hawkins S, Neutelings G.** Glycosylation Is a Major Regulator of  
928 Phenylpropanoid Availability and Biological Activity in Plants. *Frontiers in Plant Science.* 2016:  
929 710. http://doi. 3389/fpls.2016.00735

930 **Lescot M, Dehais P, Thijs G, Marchal K, Moreau Y, Van De Peer Y, Rouze P, Rombauts S.**  
931 PlantCARE, a database of plant cis-acting regulatory elements and a portal to tools for in silico  
932 analysis of promoter sequences. *Nucleic Acids Res.* 2002; **30**(1): 325-327. <http://doi.org/10.1093/nar/30.1.325>

934 **Li Y, Baldauf S, Lim EK, Bowles DJ.** Phylogenetic analysis of the UDP-glycosyltransferase multigene  
935 family of *Arabidopsis thaliana*. *J. Biol. Chem.* 2001; **276**(6): 4338-4343. <http://doi.org/10.1074/jbc.M007447200>

937 **Liu B, Raeth T, Beuerle T, Beerhues L.** A novel 4-hydroxycoumarin biosynthetic pathway. *Plant Mol.*  
938 *Biol.* 2010; **72**(1-2): 17-25. <http://doi.org/10.1007/s11103-009-9548-0>

939 **Liu X, Wu R, Bulley SM, Zhong C, Li D.** Kiwifruit MYBS1-like and GBF3 transcription factors  
940 influence L-ascorbic acid biosynthesis by activating transcription of *GDP-L-galactose*  
941 *phosphorylase 3*. *New Phytol.* 2022a; **234**(5): 1782. <http://doi.org/10.1111/nph.18097>

942 **Liu X, Zhang P, Zhao Q, Huang AC.** Making small molecules in plants: A chassis for synthetic biology-  
943 based production of plant natural products. *J. Integr. Plant Biol.* 2022b; **65**: 417-443.

944 **Luo K, Jahufer MZZ, Zhao H, Zhang R, Wu F, Yan Z, Zhang J, Wang Y, Zhang J.** Genetic improvement of  
945 key agronomic traits in *Melilotus albus*. *Crop Sci.* 2018; **58**(1): 285-294. <http://doi.org/10.2135/cropsci2017.08.0495>

947 **Luo K, Wu F, Zhang D, Dong R, Fan Z, Zhang R, Yan Z, Wang Y, Zhang J.** Transcriptomic profiling  
948 of *Melilotus albus* near-isogenic lines contrasting for coumarin content. *Sci. Rep.* 2017; **7**: 4577.  
949 <http://doi.org/10.1038/s41598-017-04111-y>

950 **Mitsuda N, Ohme-Takagi M.** Functional analysis of transcription factors in *Arabidopsis*. *Plant Cell*  
951 *Physiol.* 2009; **50**(7): 1232-1248. <http://doi.org/10.1093/pcp/pcp075>

952 **Nair RM, Whittall A, Hughes SJ, Craig AD, Revell DK, Miller SM, Powell T, Auricht GC.** Variation  
953 in coumarin content of *Melilotus* species grown in South Australia. *N. Z. J. Agric. Res.* 2010;  
954 **53**(3): 201-213. <http://doi.org/10.1080/00288233.2010.495743>

955 **Nguyen CX, Paddock KJ, Zhang Z, Stacey MG.** GmKIX8-1 regulates organ size in soybean and is the  
956 causative gene for the major seed weight QTL qSw17-1. *New Phytol.* 2021; **229**(2): 920-934.  
957 <http://doi.org/10.1111/nph.16928>

958 **Osmani SA, Bak S, Imbert A, Olsen CE, Møller BL.** Catalytic Key Amino Acids and UDP-Sugar  
959 Donor Specificity of a Plant Glucuronosyltransferase, UGT94B1: Molecular Modeling  
960 Substantiated by Site-Specific Mutagenesis and Biochemical Analyses. *Plant Physiol.* 2008;  
961 **148**(3): 1295-1308. <http://doi.org/10.1104/pp.108.128256>

962 **Osmani SA, Bak S, Møller BL.** Substrate specificity of plant UDP-dependent glycosyltransferases  
963 predicted from crystal structures and homology modeling. *Phytochemistry.* 2009; **70**(3): 325-  
964 347. <http://doi.org/10.1016/j.phytochem.2008.12.009>

965 **Patel M, Fatnani D, Parida AK.** Silicon-induced mitigation of drought stress in peanut genotypes  
966 (*Arachis hypogaea* L.) through ion homeostasis, modulations of antioxidative defense system,  
967 and metabolic regulations. *Plant Physiol. Biochem.* 2021; **166**: 290-313. <http://doi.org/10.1016/j.plaphy.2021.06.003>

969 **Perkowska I, Potrykus M, Siwinska J, Siudem D, Lojkowska E, Ihnatowicz A.** Interplay between  
970 coumarin accumulation, iron deficiency and plant resistance to *Dickeya* spp. *Int. J. Mol. Sci.*  
971 2021; **22**(12): 10. <http://doi.org/10.3390/ijms22126449>

972 **Qin W, Liu C, Jiang W, Xue Y, Wang G, Liu S.** A coumarin analogue NFA from endophytic  
973 *Aspergillus fumigatus* improves drought resistance in rice as an antioxidant. *BMC Microbiol.*

974 2019: **19**: 10. <http://doi.1186/s12866-019-1419-5>

975 **Rangani J, Panda A,Parida AK.** Metabolomic study reveals key metabolic adjustments in the  
976 xerohalophyte *Salvadora persica* L. during adaptation to water deficit and subsequent recovery  
977 conditions. *Plant Physiol. Biochem.* 2020: **150**: 180-195. <http://doi.10.1016/j.plaphy.2020.02.036>

978 **Rehman HM, Nawaz MA, Shah ZH, Ludwig-Mueller J, Chung G, Ahmad MQ, Yang SH, Lee SI.**  
979 Comparative genomic and transcriptomic analyses of Family-1 UDP glycosyltransferase in  
980 three *Brassica* species and *Arabidopsis* indicates stress-responsive regulation. *Sci. Rep.* 2018:  
981 **8**: 1875. <http://doi.10.1038/s41598-018-19535-3>

982 **Ricardo Perez-Diaz J, Perez-Diaz J, Madrid-Espinoza J, Gonzalez-Villanueva E, Moreno Y, Ruiz-  
983 Lara S.** New member of the R2R3-MYB transcription factors family in grapevine suppresses  
984 the anthocyanin accumulation in the flowers of transgenic tobacco. *Plant Mol. Biol.* 2016: **90**(1-  
985 2): 63-76. <http://doi.10.1007/s11103-015-0394-y>

986 **Robe K, Conejero G, Gao F, Lefebvre-Legendre L, Sylvestre-Gonon E, Rofidal V, Hem S, Rouhier  
987 N, Barberon M, Hecker A, et al.** Coumarin accumulation and trafficking in *Arabidopsis*  
988 *thaliana*: a complex and dynamic process. *New Phytol.* 2021: **229**(4): 2062-2079.  
989 <http://doi.1111/nph.17090>

990 **Schenke D, Boettcher C, Scheel D** Crosstalk between abiotic ultraviolet-B stress and biotic (flg22) stress  
991 signalling in *Arabidopsis* prevents flavonol accumulation in favor of pathogen defence  
992 compound production. *Plant cell and environment*, 2011: **34**(11): 1849-1864.

993 **Shao H, He XZ, Achtnine L, Blount JW, Dixon RA, Wang XQ.** Crystal structures of a multifunctional  
994 triterpene/flavonoid glycosyltransferase from *Medicago truncatula*. *Plant Cell.* 2005: **17**(11):  
995 3141-3154. <http://doi.10.1105/tpc.105.035055>

996 **Sharma A, Shahzad B, Rehman A, Bhardwaj R, Landi M, Zheng B.** Response of phenylpropanoid  
997 pathway and the role of polyphenols in plants under abiotic stress. *Molecules.* 2019: **24**(13):  
998 <http://doi.10.3390/molecules24132452>

999 **Song C, Haertl K, Mcgraphery K, Hoffmann T, Schwab W.** Attractive but toxic: emerging roles of  
1000 glycosidically bound volatiles and glycosyltransferases involved in their formation. *Molecular  
1001 Plant.* 2018: **11**(10): 1225-1236. <http://doi.10.1016/j.molp.2018.09.001>

1002 **Song C, Zhao S, Hong X, Liu J, Schulenburg K, Schwab W.** A UDP-glucosyltransferase functions in  
1003 both acylphloroglucinol glucoside and anthocyanin biosynthesis in strawberry (*Fragaria x  
1004 ananassa*). *Plant J.* 2016: **85**(6): 730-742. <http://doi.10.1111/tpj.13140>

1005 **Stringlis IA, De Jonge R, Pieterse CM.** The age of coumarins in plant-microbe interactions. *Plant Cell  
1006 Physiology.* 2019: **60**(7): 1405-1419. <http://doi.10.1093/pcp/pcz076>

1007 **Stringlis IA, Yu K, Feussner K, De Jonge R, Van Bentum S, Van Verk MC, Berendsen RL, Bakker  
1008 PaHM, Feussner I, Pieterse CMJ.** MYB72-dependent coumarin exudation shapes root  
1009 microbiome assembly to promote plant health. *Proc. Natl. Acad. Sci. U. S. A.* 2018: **115**(22):  
1010 E5213-E5222. <http://doi.10.1073/pnas.1722335115>

1011 **Sun G, Strebl M, Merz M, Blamberg R, Huang F-C, Mcgraphery K, Hoffmann T, Schwab W.**  
1012 Glucosylation of the phytoalexin *N*-feruloyl tyramine modulates the levels of pathogen-  
1013 responsive metabolites in *Nicotiana benthamiana*. *Plant J.* 2019: **100**(1): 20-37. <http://doi.10.1111/tpj.14420>

1014 **Sun Y, Ji K, Liang B, Du Y, Jiang L, Wang J, Kai W, Zhang Y, Zhai X, Chen P.** Suppressing ABA  
1015 uridine diphosphate glucosyltransferase (*Sl UGT 75C1*) alters fruit ripening and the stress  
1016 response. *Plant Physiol.* 2019: **179**(1): 100-113. <http://doi.10.1104/pp.18.09350>

1017

1018 response in tomato. *Plant J.* 2017; **91**(4): 574-589. <http://doi.10.1111/tpj.13588>

1019 **Tiwari P, Sangwan RS, Sangwan NS, JBA.** Plant secondary metabolism linked glycosyltransferases: an  
1020 update on expanding knowledge and scopes. 2016; **34**(5): 714-739.  
1021 <http://doi.10.1016/j.biotechadv.2016.03.006>

1022 **Tognetti VB, Van Aken O, Morreel K, Vandebroucke K, Van De Cotte B, De Clercq I, Chiwocha**  
1023 **S, Fenske R, Prinsen E, Boerjan W, et al.** Perturbation of indole-3-butyric acid homeostasis  
1024 by the UDP-glucosyltransferase UGT74E2 modulates *Arabidopsis* architecture and water stress  
1025 tolerance. *Plant Cell.* 2010; **22**(8): 2660-2679. <http://doi.10.1105/tpc.109.071316>

1026 **Tsai HH, Schmidt W.** Mobilization of Iron by Plant-Borne Coumarins. *Trends Plant Sci.* 2017; **22**(6):  
1027 538-548. <http://doi.10.1016/j.tplants.2017.03.008>

1028 **Vanholme R, Sundin L, Seetso KC, Kim H, Liu X, Li J, De Meester B, Hoengenaert L, Goeminne**  
1029 **G, Morreel K, et al.** COSY catalyses trans-cis isomerization and lactonization in the  
1030 biosynthesis of coumarins. *Nature Plants.* 2019; **5**(10): 1066-1075. <http://doi.10.1038/s41477-019-0510-0>

1032 **Voges MJ, EEE, Bai Y, Schulze-Lefert P, Sattely ES.** Plant-derived coumarins shape the composition  
1033 of an *Arabidopsis* synthetic root microbiome. *Proc. Natl. Acad. Sci. U. S. A.* 2019; **116**(25):  
1034 12558-12565. <http://doi.10.1073/pnas.1820691116>

1035 **Wang S, Duan Z, Zhang J.** Establishment of hairy root transformation system of *Melilotus albus*  
1036 induced by *Agrobacterium rhizogenes*. *Acta Agrestia Sinica.* 2021; **29**(11): 2591-2599.

1037 **Wang W.** The molecular detection of corynespora cassiicola on cucumber by PCR assay using DNAMan  
1038 software and NCBI. In International conference on computer and computing technologies in  
1039 agriculture: Springer, 2015: 248-258

1040 **Wu F, Duan Z, Xu P, Yan Q, Meng M, Cao M, Jones CS, Zong X, Zhou P, Wang Y, et al.** Genome  
1041 and systems biology of *Melilotus albus* provides insights into coumarins biosynthesis. *Plant*  
1042 *Biotechnol. J.* 2022; **23**(4): 592-609. <http://doi.10.1111/pbi.13742>

1043 **Wu F, Luo K, Yan Z, Zhang D, Yan Q, Zhang Y, Yi X, Zhang J.** Analysis of miRNAs and their target  
1044 genes in five *Melilotus albus* NILs with different coumarin content. *Sci. Rep.* 2018; **8**: 14138.  
1045 <http://doi.10.1038/s41598-018-32153-3>

1046 **Yang YL, Zhou H, Du G, Feng KN, Feng T, Fu XL, Liu JK, Zeng Y.** A Monooxygenase from  
1047 *Boreostereum vibrans* Catalyzes Oxidative Decarboxylation in a Divergent Vibralactone  
1048 Biosynthesis Pathway. *Angewandte Chemie-International Edition.* 2016; **55**(18): 5463-5466.  
1049 <http://doi.10.1002/anie.201510928>

1050 **Zabala JM, Marinoni L, Giavedoni JA, Schrauf GE.** Breeding strategies in *Melilotus albus* Desr., a  
1051 salt-tolerant forage legume. *Euphytica.* 2018; **214**(2): 22. <http://doi.10.1007/s10681-017-2031-0>

1053 **Zhang J, Di H, Luo K, Jahufer Z, Wu F, Duan Z, Stewart A, Yan Z, Wang Y.** Coumarin content,  
1054 morphological variation, and molecular phylogenetics of *Melilotus*. *Molecules.* 2018; **23**(4):  
1055 810. <http://doi.10.3390/molecules23040810>

1056 **Zhang S-Y, Meng L, Gao W-Y, Song N-N, Jia W, Duan H-Q** Advances on biological activities of  
1057 coumarins. *Chin Pharm J.* 2005; **30**(6): 410-414.

1058 **Zhang Z, Jin X, Liu Z, Zhang J, Liu W.** Genome-wide identification of *FAD* gene family and functional  
1059 analysis of *MsFAD3.1* involved in the accumulation of alpha-linolenic acid in alfalfa. *Crop Sci.*  
1060 2021; **61**(1): 566-579. <http://doi.10.1002/csc2.20362>

1061 **Zhao J, Zhang W, Zhao Y, Gong X, Guo L, Zhu G, Wang X, Gong Z, Schumaker KS, Guo Y.** SAD2,

1062 an importin beta-like protein, is required for UV-B response in *Arabidopsis* by mediating MYB4  
1063 nuclear trafficking. *Plant Cell*. 2007; **19**(11): 3805-3818. <http://doi.10.1105/tpc.106.048900>

1064 **Zheng H, Jing L, Jiang X, Pu C, Zhao S, Yang J, Guo J, Cui G, Tang J, Ma Y, et al.** The ERF-VII  
1065 transcription factor SmERF73 coordinately regulates tanshinone biosynthesis in response to  
1066 stress elicitors in *Salvia miltiorrhiza*. *New Phytol*. 2021; **231**(5): 1940-1955. <http://doi.10.1111/nph.17463>

1068 **Zong X, Wang S, Han Y, Zhao Q, Xu P, Yan Q, Wu F, Zhang J.** Genome-wide profiling of the  
1069 potential regulatory network of lncRNA and mRNA in *Melilotus albus* under salt stress. *Environ.*  
1070 *Exp. Bot.* 2021; **189**: 104548. <http://doi.10.1016/j.envexpbot.2021.104548>

1071 **Figure legends**

1072 **Figure 1** Discovery of a specific scopoletin UDP-glycosyltransferase in *M. albus*. A)  
1073 Scopolin content in root, stem and leaf tissues of 2-month-old plants at the flowering  
1074 stage of the two NILs, JiMa46 and JiMa49. The error bars indicate the SD values from  
1075 at least three repetitions. Significant differences were detected by Student's t-test: \*\*,  
1076  $P<0.01$ . B) Identification and localization of the scopolin biosynthesis locus between  
1077 the two NILs based on BSA. The annotated gene was identified with SNPs and InDels  
1078 between NILs JiMa46 and JiMa49. Each point represents an individual SNP locus. C)  
1079 Physical position, gene structure, polymorphisms between JiMa46 and JiMa49 of  
1080 *Malbus0502448.1*. Mutational changes in JiMa49 are indicated. Exon and the highly  
1081 conserved plant secondary product glycosyltransferases (PSPG) box of plant  
1082 glycosyltransferases are indicated in grey and black boxes, respectively. Nucleotide  
1083 polymorphisms are indicated at their corresponding positions in the coding sequences.

1084 **Figure 2** Amino acid sequence alignment, phylogenetic analysis, subcellular  
1085 localization of MaUGT79. A) Amino acid alignments of MaUGT79 with other  
1086 identified UDP-glycosyltransferase (UGT) proteins involved in coumarin biosynthesis  
1087 including AtUGT73B3, AtUGT73B4, NtGT3, NtGT1a, TOGT1, FaGT6 and FaGT7.  
1088 The red arrow at the N-terminus indicates the presence of a critical catalytic His that is  
1089 universally conserved across all plant UGTs. A neighboring residue, believed to be  
1090 important in contributing to sugar donor recognition, is indicated by the green arrow.  
1091 The black rectangle at the C-terminus indicates the domains of the PSPG box. Numbers  
1092 indicate the last residue in each line. Identical residues are highlighted by a black

1093 background and similar residues are highlighted by a grey background. The red dots  
1094 indicate MaUGT79. B) Phylogenetic tree of MaUGT79 together with other functionally  
1095 characterized UGTs. The tree is constructed using the Neighbor-Joining method by the  
1096 MEGA X software. Numbers indicate bootstrap values for 1000 replicates. The  
1097 GenBank accession numbers of the UGT proteins are: AtUGT73B3 (AAL32831);  
1098 AtUGT73B4 (BAE99671); NtGT3 (BAB88934); NtGT1a (BAB60720); TOGT1  
1099 (AAK28303); FaGT6 (ABB92748); FaGT7 (ABB92749); AtUGT71B1 (BAB02837);  
1100 MtUGT71G1 (RHN56458); AtUGT71C1 (AAC35226); AtUGT71C4 (AAG18592);  
1101 AtUGT72B1 (AAK25972); AtUGT72E1 (AAK83619); AtUGT72E2 (BAA97275);  
1102 AtUGT72E3 (AAC26233); AtUGT89A2 (CAB83309); AtUGT89B1 (AEE35520);  
1103 AtUGT73C5 (AAD20156); AtUGT73C6 (AAD20155). The red dot indicates  
1104 MaUGT79. C) Relative expression levels of *MaUGT79* in root, stem and leaf tissues of  
1105 2-month-old plants at the flowering stage of the two NILs, JiMa46 and JiMa49. Data  
1106 are normalized by  $\beta$ -tubulin. Data are shown as the mean (n = 3), and significant  
1107 differences were detected by Student's t-test: \*, P<0.05 or \*\*, P<0.01. (d) The  
1108 subcellular localization of MaUGT79 in *N. benthamiana* leaves. *MaUGT79* was fused  
1109 to RFP. The fluorescence was observed under a confocal laser scanning microscope.  
1110 Scale bars indicate 50  $\mu$ m.

1111 **Figure 3** The *in vitro* glucosylating activity of MaUGT79 toward different coumarins.  
1112 HPLC analyses of the reaction products catalyzed by fusion protein MaUGT79 with *o*-  
1113 coumaric acid A), umbelliferone B), esculetin C), scopoletin D) compared with  
1114 authentic standards. UDP-glucose was used as the sugar donor. Empty vector was used  
1115 as a negative control. The authentic *o*-coumaric acid, umbelliferone, esculetin, scopolin  
1116 and scopoletin were used as the standards.

1117 **Figure 4** Over- or knockdown expression of *MaUGT79* alters scopolin content in *M.*  
1118 *albus* hairy roots. A) Analysis of *MaUGT79* expression levels and B) scopolin content  
1119 in control (EV), overexpression (OE) and RNAi transgenic hairy roots. C) Gene  
1120 expression levels of four scopolin biosynthesis genes (*4CL1*, *CCoAOMT1*, *F6'H1*, and

1121 *BGLU42*) in 21-d-old hairy roots. qRT-PCR was performed to detect gene expression  
1122 levels. Data are normalized by  $\beta$ -tubulin. Data are shown as the mean (n=3). The error  
1123 bars indicate the SD values from at least three repetitions. Significant differences were  
1124 detected by Student's t-test: \*,  $P < 0.05$  or \*\*,  $P < 0.01$ .

1125 **Figure 5** *MaUGT79* positively regulates drought tolerance in *M. albus* hairy roots. A)  
1126 Drought stress tolerance analysis of *MaUGT79* in a yeast expression system compared  
1127 with empty vector pYES2 (control) yeast. The two yeast cultures were independently  
1128 grown in synthetic complete (SC)-Ura liquid medium containing 2% (m/v) galactose at  
1129 30 °C for 36 h up to  $A_{600}=0.4$ . Then, the yeast was collected and adjusted with SC-Ura  
1130 including 2% galactose and cultivated up to  $A_{600}=1$  for stress analysis. The same  
1131 number of cells was resuspended in 30% PEG6000. Then, serial dilutions ( $10^0$ ,  $10^{-1}$ ,  
1132  $10^{-2}$ ,  $10^{-3}$ ,  $10^{-4}$ ,  $10^{-5}$ ) were spotted onto SC-Ura agar plates and incubated at 30°C for 3  
1133 d. As a control, yeast with  $A_{600}=1$  without any stress was also spotted onto SC-Ura agar  
1134 plates with the same dilutions as the treatments and grown at 30 °C for 3 d. B)  
1135 Phenotypes of single seedling of overexpressing *MaUGT79* transgenic hairy roots (OE-  
1136 *MaUGT79*), RNAi-*MaUGT79* transgenic hairy roots and transgenic hairy roots  
1137 containing an empty vector (EV) grown under normal and 30% PEG6000 treatment for  
1138 3 days. C) Histochemical staining with NBT in hairy roots of EV and OE-*MaUGT79*  
1139 under normal and 30% PEG6000 treatment for 3 days. (d-g) MDA content D),  $O_2^-$   
1140 content E),  $H_2O_2$  content F) and scopolin content G) in hairy roots of EV, OE-  
1141 *MaUGT79* and RNAi-*MaUGT79* under normal and 30% PEG6000 treatment for 3 days.  
1142 H) Phenotypes of single plant with OE-*MaUGT79*, RNAi-*MaUGT79* and EV  
1143 transgenic hairy roots grown under normal and drought stress for 22 days. I) Relative  
1144 water content of the plants with OE-*MaUGT79*, RNAi-*MaUGT79* and EV transgenic  
1145 hairy roots under normal and drought stress at 22 days J), Survival rates of the plants  
1146 with OE-*MaUGT79*, RNAi-*MaUGT79* and EV transgenic hairy roots grown under  
1147 drought stress at 22 days, K-N) scopolin content K), MDA content L),  $O_2^-$  content M),  
1148  $H_2O_2$  content N) in hairy roots of EV, OE-*MaUGT79* and RNAi-*MaUGT79* grown  
1149 under normal and drought stress for 22 days. The error bars indicate the SD values from

1150 at least three repetitions of each treatment. Asterisks indicate significant differences  
1151 between EV, OE-*MaUGT79* and RNAi-*MaUGT79* under the same growth conditions.  
1152 Significant differences were detected by Student's t-test: \*,  $P<0.05$  or \*\*,  $P<0.01$ .

1153 **Figure 6** The promoter of *MaUGT79* is the direct target of MaMYB4 (MYB,  
1154 myeloblastosis). A) Schematic diagram of the bait fragments (P1 to P5) used to  
1155 construct the reporter vectors in the yeast one-hybrid assay. The red triangles indicate  
1156 MBY biding sites. B) Schematic diagram of the prey plasmid and bait plasmid in yeast  
1157 one-hybrid (Y1H) assay. The promoter fragment of *MaUGT79* was cloned into the  
1158 pAbAi vector to generate the bait plasmid and the prey plasmid was generated by  
1159 recombining the MaMYB4 gene into the pGADT7 vector. C) Transcriptional activation  
1160 analysis of Y1H Gold [*Pro1/2/3/4/5/MaUGT79-pAbAi*]. D) Yeast one-hybrid assay. A  
1161 pair of plasmids, pAbAi containing different fragments of the *MaUGT79* promoter and  
1162 pGADT7 containing MaMYB4 were introduced into yeast strain Y1H gold and  
1163 cultured on SD medium without Leu containing different concentrations of AbA at  
1164 30°C for 3 days. E) Schematic diagram of the reporter plasmid and effector plasmid.  
1165 The promoter fragment of *MaUGT79* was cloned into the pGreenII 0800-LUC vector  
1166 to generate the reporter plasmid. The effector plasmid was generated by recombining  
1167 the MaMYB4 gene into an overexpression vector (pBI 121). F) Dual-luciferase (LUC)  
1168 assay in *N. benthamiana* leaves showing that MaMYB4 activates transcription of  
1169 *MaUGT79* promoters. The leaves infiltrated with the empty vector and  
1170 *MaUGT79pro::LUC* as a control. Representative photographs were taken (above), and  
1171 LUC/Renilla Luciferase (REN) activity detection to verify that MaMYB4 activates the  
1172 transcription of *MaUGT79* (below). The error bars indicate the SD values from the  
1173 mean of at least five repetitions. Significant differences were detected by Student's t-  
1174 test: \*,  $P<0.05$ .

1175 **Figure 7** MaMYB4 positively regulates scopolin content in *M. albus* hairy roots. (MYB,  
1176 myeloblastosis). A-B) Quantitative reverse-transcription (qRT)-PCR analysis of  
1177 MaMYB4 A) and *MaUGT79* B) in control (EV), OE-MaMYB4 and RNAi-MaMYB4

1178 transgenic hairy roots. C) Scopolin content in control (EV), OE-MaMYB4 and RNAi-  
1179 MaMYB4 transgenic hairy roots. D) Gene expression levels of four scopolin  
1180 biosynthesis genes (*4CL1*, *CCoAOMT1*, *F6'H1*, and *BGLU42*) in 21-d-old hairy roots.  
1181 qRT-PCR was performed to detect gene expression levels. Data are normalized by  $\beta$ -  
1182 *tubulin*. The error bars indicate the SD values from the mean of at least three repetitions.  
1183 Significant differences were detected by Student's t-test: \*,  $P<0.05$  or \*\*,  $P<0.01$ .

1184 **Figure 8** MaMYB4 positively regulates drought tolerance in *M. albus* hairy roots. A)  
1185 Phenotypes of single seedling of overexpressing MaMYB4 transgenic hairy roots (OE-  
1186 MaMYB4), RNAi-MaMYB4 transgenic hairy roots and transgenic hairy roots  
1187 transferring an empty vector (EV) under normal and 30% PEG6000 treatment for 3  
1188 days. B-C) Histochemical staining with NBT B) and DAB C) in hairy roots of EV, OE-  
1189 MaMYB4 and RNAi-MaMYB4 under normal and 30% PEG6000 treatment for 3 days.  
1190 D-G) MDA content D),  $H_2O_2$  content E),  $O_2^-$  content F) and *MaUGT79* expression level  
1191 G) in hairy roots of EV, OE-MaMYB4 and RNAi- MaMYB4 under normal and 30%  
1192 PEG6000 treatment for 3 days. H) Phenotypes of single plants with OE-MaMYB4,  
1193 RNAi- MaMYB4 and EV transgenic hairy roots under normal and drought stress for  
1194 22 days. I) Relative water content of plants with OE- MaMYB4, RNAi- MaMYB4 and  
1195 EV transgenic hairy roots under normal and drought stress at 22 days J), Survival rates  
1196 of plants with OE-MaMYB4, RNAi-MaMYB4 and EV transgenic hairy roots grown  
1197 under drought stress at 22 days, K-N) scopolin content K), MDA content L),  $O_2^-$  content  
1198 M),  $H_2O_2$  content N) in hairy roots of EV, OE-MaMYB4 and RNAi-MaMYB4 grown  
1199 under normal and drought stress for 22 days. The error bars indicate the SD values from  
1200 at least three repetitions of each treatment. Asterisks indicate significant differences  
1201 between EV, OE-MaMYB4 and RNAi-MaMYB4 under the same growth conditions.  
1202 Significant differences were detected by Student's t-test: \*,  $P<0.05$  or \*\*,  $P<0.01$ .

1203 **Figure 9** A proposed mechanistic model for the drought-dependent regulation of  
1204 scopolin biosynthetic *MaUGT79* gene expression, regulated by MaMYB4 in *M. albus*.  
1205 Under drought conditions, MaMYB4 is up-regulated and activates the expression of

1206 *MaUGT79*. *MaUGT79* catalyses the conversion of scopoletin to scopolin, which results  
1207 in an increase in scopolin content. The accumulation of scopolin leads to drought  
1208 tolerance by increasing ROS scavenging.